doi:10.1093/scan/nst106 SCAN (2014) 9, 1289–1302

Informatic parcellation of the network involved in the computation of subjective value

John A. Clithero[1] and Antonio Rangel[1,2]
[1]Division of the Humanities and Social Sciences and [2]Computation and Neural Systems, California Institute of Technology, Pasadena, CA 91125, USA

Understanding how the brain computes value is a basic question in neuroscience. Although individual studies have driven this progress, meta-analyses provide an opportunity to test hypotheses that require large collections of data. We carry out a meta-analysis of a large set of functional magnetic resonance imaging studies of value computation to address several key questions. First, what is the full set of brain areas that reliably correlate with stimulus values when they need to be computed? Second, is this set of areas organized into dissociable functional networks? Third, is a distinct network of regions involved in the computation of stimulus values at decision and outcome? Finally, are different brain areas involved in the computation of stimulus values for different reward modalities? Our results demonstrate the centrality of ventromedial prefrontal cortex (VMPFC), ventral striatum and posterior cingulate cortex (PCC) in the computation of value across tasks, reward modalities and stages of the decision-making process. We also find evidence of distinct subnetworks of co-activation within VMPFC, one involving central VMPFC and dorsal PCC and another involving more anterior VMPFC, left angular gyrus and ventral PCC. Finally, we identify a posterior-to-anterior gradient of value representations corresponding to concrete-to-abstract rewards.

Keywords: decision making; fMRI; IBMA; meta-analysis; value

INTRODUCTION

Over the last few years, there has been a large effort to identify the computations made by the brain when executing different types of decisions, and when evaluating the outcomes generated by those decisions. There is a growing consensus that the assignment of values to stimuli is a critical part of both processes (Rangel *et al.*, 2008; Glimcher, 2011; Grabenhorst and Rolls, 2011; Rushworth *et al.*, 2011, Wallis, 2012), and that the ventromedial prefrontal cortex (VMPFC) plays a critical role in the computation of value both at decision and outcome (Rangel and Hare, 2010; Padoa-Schioppa, 2011; Levy and Glimcher, 2012).

One of the fundamental goals of this research program is to identify networks that are involved in the computation of value whenever that variable is needed. Measures of value can be computed for different types of rewards, for different purposes and at different stages, such as decision and outcome. Clearly, in order to answer these questions, it is necessary to collect and compare data in many different decision-making paradigms. This makes it challenging for single studies to adequately answer these questions, as the vast majority of studies address the computation of value in the context of a specific choice paradigm with a specific reward modality. Some insight can be gained by carrying out qualitative reviews of the literature (Rangel *et al.*, 2008; Glimcher, 2011; Grabenhorst and Rolls, 2011; Padoa-Schioppa, 2011; Rushworth *et al.*, 2011), but the ideal methodology involves the use of meta-analyses (Kober and Wager, 2010; Yarkoni *et al.*, 2010).

We take an informatic approach to understanding value computation in the brain, by conducting several meta-analyses of over 80 functional magnetic resonance imaging (fMRI) papers related to the computation of value. Our goal is to address the following open questions. First, what is the full set of brain regions that reliably correlate with stimulus values when they need to be computed across tasks and reward modalities? Second, is this set of regions organized into dissociable functional networks across tasks and reward modalities? Third, is a distinct set of areas involved in the computation of stimulus values at decision and outcome? Fourth, are different regions involved in the computation of stimulus values for different reward modalities (e.g. food *vs* money)?

The study adds to previous uses of meta-analytic tools to understand the neurobiology of decision making, but differs in important ways. Several studies (Peters and Buchel, 2010b; Grabenhorst and Rolls, 2011; Levy and Glimcher, 2012; Liu *et al.*, 2011) also investigate the computation of value, but do not present a comprehensive analysis of the existing literature and focus primarily on the VMPFC. Another recent meta-analysis looks at fMRI studies of subjective pleasantness (Kuhn and Gallinat, 2012), but their focus is exclusively on the time of reward receipt. Two other meta-analyses focus on specific decision environments, such as intertemporal choice (Carter *et al.*, 2010) and risky choice (Mohr *et al.*, 2010). In contrast, here we look at the entire body of published papers related to the computation of value, regardless of task, reward modality or stage of processing. In addition, we seek to delineate the properties of the valuation network beyond the VMPFC.

METHODS

Study selection for coordinate-based meta-analysis

Most of the analyses performed in the study involve coordinate-based meta-analysis (CBMA), a common methodology (Salimi-Khorshidi *et al.*, 2009; Kober and Wager, 2010; Eickhoff *et al.*, 2012). The studies selected for analysis were identified as follows. We started with PubMed searches (6 July 2012) to construct an initial candidate set that required the following keywords to be found in the title or abstract of scientific articles: ('reward*' OR '*economic*') AND ('preference*' OR 'value*' OR 'utility' OR 'valuation*') AND ('functional' AND 'magnetic' AND 'resonance' AND 'imaging') OR 'fMRI' OR 'neuroimaging' OR 'neural' OR 'brain*') AND ('pay*' OR 'purchase*' OR 'buy*' OR 'decision*' OR 'decide*' OR 'choice*' OR 'choose*'). This initial query yielded 503 results, and was

Received 22 February 2013; Revised 24 April 2013; Accepted 16 July 2013
Advance Access publication 24 July 2013
We acknowledge funding from the National Science Foundation, the Lipper Foundation and the Gordon and Betty Moore Foundation.
Correspondence should be addressed to John A. Clithero, Division of the Humanities and Social Sciences, MC 228-77, California Institute of Technology, Pasadena, CA 91125, USA. E-mail: clithero@hss.caltech.edu

supplemented by fMRI papers cited by recent review articles (Grabenhorst and Rolls, 2011; Padoa-Schioppa, 2011; Rushworth *et al.*, 2011), but not recovered by the search. All non-relevant results (e.g. rodent studies that passed all the term searches in PubMed) were first removed from the list. We then manually removed all papers that did not satisfy one or more of the following necessary criteria for inclusion: (i) fMRI study of healthy human individuals, (ii) whole-brain analyses reported, (iii) parametric contrasts of subjective value reported (e.g. not just simply 'high' *vs* 'low' value) and (iv) peak-activation coordinates reported. This lead to the final corpus of 81 fMRI studies (Table 1). As the majority of the studies only reported positive (but not negative) correlations with value signals, we focus almost exclusively on the analysis of the positive contrasts.

Statistical inference for coordinate-based meta-analysis

For CBMA, we employed the widely used activation likelihood estimation (ALE) method (Laird *et al.*, 2005; Eickhoff *et al.*, 2012; Fox and Friston, 2012; Turkeltaub *et al.,* 2012). Intuitively, the goal is to test against the null hypothesis that the foci of activation reported in the corpus of studies are uniformly distributed across the brain, as opposed to concentrated in some regions (Eickhoff *et al.,* 2012). The method is based on the idea that peak locations of activation are observed with noise in each study, but that the distribution of true locations from which they are observed is fixed across studies.

A meta-analysis employing the ALE statistic is carried out in several steps. First, for each included study, a map of the activation likelihood (commonly referred to as a modeled activation map, or MA) is computed. In this step, the probability of activation at any voxel is assumed to be a function of: (i) the Euclidean distance between the reported peak coordinates and the voxel, (ii) the volume of the voxel (here, 8 mm^3) and (iii) the spatial uncertainty associated with the reported peak coordinates. So, the MA statistic for a contrast i at voxel v denotes the probability that at least one true peak of activation lies within the voxel v in that contrast. Second, the MA maps are aggregated across contrasts to compute the ALE score for each voxel v. This is done by taking the probabilistic union of the MA statistic across all contrasts for each voxel. The ALE statistic denotes the probability that at least one true peak of activation lies in the voxel across the population of all possible studies. Third, a permutation test (described below) is used to identify voxels in which the ALE statistic is higher than expected by mere chance. More details on how the ALE statistic is computed are outlined by its developers (Laird *et al.,* 2005; Eickhoff *et al.,* 2009, 2012; Turkeltaub *et al.,* 2012).

Importantly, our analyses used a recent version of ALE that accounts for heterogeneity in spatial uncertainty across studies (Eickhoff *et al.,* 2009, 2012; Fox and Friston, 2012; Turkeltaub *et al.,* 2012) as well as for heterogeneity in authors' tendency to report multiple or single peak coordinates per cluster of activation (Turkeltaub *et al.,* 2012). This allows random-effects estimates of ALE, meaning the results are generalizable beyond the studies in the corpus (Eickhoff *et al.,* 2009). Each of our ALE analyses was carried out using the GingerALE package (http://brainmap.org/ale/), which incorporates these improvements.

First, we computed ALE maps for single contrasts of interest (e.g. to identify regions that correlate with a specific type of value across studies). Each of these ALE maps were thresholded with a voxel-level requirement of $P < 0.001$ and a cluster-level requirement of $P < 0.05$, depicted in the figures and summarized in the tables. The significance of the ALE values was determined as follows. The ALE statistics in each voxel were compared with a null distribution of ALE values generated from 10 000 permutations (Eickhoff *et al.,* 2009, 2012). Each permutation involved constructing an ALE value for all voxels in the whole-brain gray-matter mask. For each voxel in the mask, a randomly and independently chosen voxel from each MA map was selected and the ALE value was computed for this selection. After 10 000 permutations, the estimated ALE values for the actual data were compared with this empirically generated null distribution (pooling all voxels in the whole-brain mask). This stringent threshold was applied to all ALE tests, regardless of the number of contrasts and foci used.

Second, we carried out several contrasts between two ALE maps, which provide a test against the null hypothesis that there is no difference in the spatial pattern of reported loci across studies for the two contrasts underlying those activation maps. For contrasts of ALE values, we used ALE images with voxel-level significance requirement of $P < 0.001$. This criterion constructs the set of voxels in which the statistical contrast is performed and was employed to focus inference on areas reliably identified in each initial ALE test (Eickhoff *et al.,* 2011). Differences between ALE maps were then subjected to 10 000 permutations and required a voxel-level significance of $P < 0.005$ (we also report $P < 0.001$). This procedure should effectively balance inference on reliable areas of activation without generating a bias toward false positives (Laird *et al.,* 2005; Eickhoff *et al.,* 2011).

Third, we used the ALE statistic to look for co-activation across the brain with specific regions-of-interest (ROIs). This was done by: (i) identifying reported foci within the ROI, for the contrast of interest, in the corpus of studies, (ii) identifying all other foci reported from the same contrasts in studies that also reported activation within the ROI and (iii) computing ALE statistics for the set of identified foci. Note that this third procedure is similar to the first one, except for the fact that the set of foci included is restricted by co-activation with the ROI. Thus, significant clusters of activation outside the ROI can be interpreted as areas that reliably co-activate with the ROI across studies, for the contrast of interest. A similar logic has been previously employed to identify networks using meta-analyses in other domains (Toro *et al.,* 2008; Smith *et al.,* 2009; Gilbert *et al.,* 2010; Cauda *et al.,* 2011). The ROIs used in the co-activation analysis were constructed using 9 mm radius spheres about peak coordinates of activation taken from the ALE analyses of interest.

We note that other methods have been proposed for carrying out these types of CBMA, such as kernel density analysis, or KDA (Wager *et al.,* 2003, 2007; Kober and Wager, 2010). However, both ALE and KDA are based on aggregating foci reported for any given study into a single MA map, which are then combined across studies to identify spatial convergence. A full comparison of KDA and ALE is beyond the scope of this article, but has been discussed elsewhere (Kober and Wager, 2010; Eickhoff *et al.*, 2012).

All analyses were performed in Montreal Neurological Institute (MNI) space. Coordinates from studies reported in Talairach space were converted to MNI using an algorithm available within GingerALE (Lancaster *et al.,* 2007). All coordinates reported here are in MNI space. All images of statistical brain maps were generated using MRICron (Rorden *et al.,* 2007) and the MNI-152 1 mm template.

Construction of dataset for image-based meta-analysis

When feasible, we also carried out a parallel image-based meta-analysis (IBMA). This was done using data from previously published fMRI studies including the last author of this article (Table 2). Each of the included studies provided a group-level statistical parametric map (SPM, an unthresholded *t*-statistic image) for the corresponding parametric value contrasts reported in each study. All of these analyses were completed in SPM5 or SPM8 (Friston, 2007). The remainder of the IBMA was completed using utilities from FMRIB Software Library (FSL) 4.1.8 (Woolrich *et al.,* 2009). Once provided with the *t*-statistic data and the degrees of freedom corresponding to those SPMs, we

Table 1 Included CBMA studies from PubMed searches and review articles

Number	References	Journal	Package	*N*	Outcome	Decision	Money	Food	Other
1	Anderson *et al.*, 2003	Nature Neuroscience	SPM99	16	YES	-	-	-	YES
2	Basten *et al.* (2010)	Proceedings of the National Academy of Sciences, *USA*	SPM5	19	-	YES	YES	-	-
3	Behrens *et al.*, 2008	Nature	FSL	24	-	YES	YES	-	-
4	Boorman *et al.*, 2009	Neuron	FSL	18	-	YES	YES	-	-
5	Brooks *et al.*, 2010	Frontiers in Neuroscience	SPM5	36	-	YES	-	-	YES
6	Chib *et al.*, 2009	Journal of Neuroscience	SPM5	19	-	YES	YES	YES	YES
7	Cloutier *et al.*, 2008	Journal of Cognitive Neuroscience	SPM2	48	YES	-	-	-	YES
8	Cohen, 2007	Social Cognitive and Affective Neuroscience	SPM99	17	-	YES	YES	-	-
9	Croxson *et al.*, 2009	Journal of Neuroscience	FSL	16	-	-	YES	-	-
10	Daw *et al.*, 2006	Nature	SPM2	14	YES	-	YES	-	-
11	de Araujo *et al.*, 2003	Journal of Neurophsyiology	SPM2	11	YES	-	-	YES	-
12	de Araujo *et al.*, 2005	Neuron	SPM2	12	YES	-	-	-	YES
13	De Martino *et al.*, 2009	Journal of Neuroscience	SPM2	18	-	YES	YES	-	-
14	FitzGerald *et al.*, 2009	Journal of Neurosicence	SPM5	16	-	YES	YES	YES	YES
15	FitzGerald *et al.*, 2010	Current Biology	SPM5	18	-	YES	YES	-	-
16	Glascher *et al.*, 2009	Cerebral Cortex	SPM5	20	-	YES	YES	-	-
17	Grabenhorst and Rolls, 2009	Neuroimage	SPM5	12	YES	-	-	-	YES
18	Grabenhorst *et al.*, 2010	Neuroimage	SPM5	12	YES	-	-	YES	YES
19	Hampton *et al.*, 2006	Journal of Neuroscience	SPM2	16	-	YES	YES	-	-
20	Hare *et al.*, 2008	Journal of Neuroscience	SPM5	16	-	YES	YES	YES	-
21	Hare *et al.*, 2009	Science	SPM5	37	-	YES	YES	-	-
22	Hare *et al.*, 2010	Journal of Neuroscience	SPM5	22	-	YES	-	-	YES
23	Hare *et al.*, 2011a	Journal of Neuroscience	SPM8	33	-	YES	-	YES	-
24	Hare *et al.*, 2011b	Proceedings of the National Academy of Sciences, *USA*	SPM8	19	-	YES	-	YES	-
25	Hsu *et al.*, 2009	Journal of Neuroscience	SPM2	21	-	YES	YES	-	-
26	Hutcherson *et al.*, 2012	Journal of Neuroscience	SPM5	26	-	YES	-	YES	-
27	Izuma *et al.*, 2010	Proceedings of the National Academy of Sciences, *USA*	SPM8	20	YES	-	-	YES	-
28	Janowski *et al.*, 2013	Social Cognitive and Affective Neuroscience	SPM5	32	-	YES	-	-	YES
29	Jocham *et al.*, 2011	Journal of Neuroscience	FSL	18	-	YES	YES	-	-
30	Jocham *et al.*, 2012	Nature Neuroscience	FSL	25	-	YES	YES	-	-
31	Kable and Glimcher, 2007	Nature Neuroscience	BVQX	12	-	YES	YES	-	-
32	Kable and Glimcher, 2010	Journal of Neurophsyiology	BVQX	22	-	YES	YES	-	-
33	Kang *et al.*, 2011	Journal of Neuroscience	SPM5	24	-	YES	-	-	YES
34	Kim *et al.*, 2006	PLoS Biology	SPM2	16	YES	YES	YES	-	-
35	Kim *et al.*, 2011	Cerebral Cortex	SPM2	18	YES	-	YES	YES	-
36	Knutson *et al.*, 2007	Neuron	AFNI	26	-	YES	-	-	YES
37	Koeneke *et al.*, 2008	Behavioral and Brain Functions	SPM5	19	YES	-	-	YES	-
38	Kringelbach *et al.*, 2003	Cerebral Cortex	SPM99	10	YES	-	-	YES	-
39	Lebreton *et al.*, 2009	Neuron	SPM5	20	YES	-	-	-	YES
40	Levy *et al.*, 2010	Journal of Neurophsyiology	BVQX	20	-	YES	YES	-	-
41	Levy and Glimcher, 2011	Journal of Neuroscience	BVQX	19	-	YES	YES	YES	-
42	Lim *et al.*, 2011	Journal of Neuroscience	SPM8	20	-	YES	-	YES	-
43	Lin *et al.*, 2012	Social Cognitive and Affective Neuroscience	SPM5	22	YES	-	YES	-	YES
44	Litt *et al.*, 2011	Cerebral Cortex	SPM5	20	-	YES	-	YES	-
45	Liu *et al.*, 2012	Behavioral Brain Research	BVQX	19	-	YES	YES	-	-
46	McClure *et al.*, 2004	Neuron	SPM2	15, 17	YES	-	-	YES	-
47	O'Doherty *et al.*, 2006	Neuron	SPM2	13	YES	-	-	YES	-
48	Park *et al.*, 2011	Journal of Neuroscience	SPM5	24	-	YES	YES	-	YES
49	Peters and Buchel, 2009	Journal of Neuroscience	SPM5	22, 18	-	YES	YES	-	-
50	Peters and Buchel, 2010a	Neuron	SPM5	30	-	YES	YES	-	-
51	Pine *et al.*, 2009	Journal of Neuroscience	SPM5	24	-	YES	YES	-	-
52	Pine *et al.*, 2010	Journal of Neuroscience	SPM5	12	-	YES	YES	-	-
53	Plassmann *et al.*, 2007	Journal of Neuroscience	SPM5	19	-	YES	-	YES	-
54	Plassmann *et al.*, 2008	Proceedings of the National Academy of Sciences, *USA*	SPM5	20	YES	-	-	YES	-
55	Plassmann *et al.*, 2010	Journal of Neuroscience	SPM5	19	-	YES	-	YES	-
56	Prevost *et al.*, 2010	Journal of Neuroscience	SPM5	16	-	YES	-	-	YES
57	Rolls and McCabe, 2007	European Journal of Neuroscience	SPM2	8	YES	-	-	YES	-
58	Rolls *et al.*, 2008	Neuroimage	SPM5	12	YES	-	-	-	YES
59	Rolls *et al.*, 2010	Journal of Cognitive Neuroscience	SPM5	12	YES	-	-	-	YES
60	Serences, 2008	Neuron	BVQX	14	-	YES	YES	-	-
61	Sescousse *et al.*, 2010	Journal of Neuroscience	SPM2	17	YES	-	YES	-	YES
62	Shenhav and Greene, 2010	Neuron	SPM2	34	-	YES	-	-	YES
63	Simon and Daw, 2011	Journal of Neuroscience	SPM5	18	-	YES	YES	-	-
64	Smith *et al.*, 2010	Journal of Neuroscience	FSL	23	YES	-	YES	-	YES
65	Sokol-Hessner *et al.*, 2012	European Journal of Neuroscience	SPM8	22	-	YES	-	YES	-
66	Sripada *et al.*, 2011	Human Brain Mapping	SPM2	20	-	YES	YES	-	-

(continued)

Table 1 Continued

Number	References	Journal	Package	*N*	Outcome	Decision	Money	Food	Other
67	Studer *et al.*, 2012	Frontiers in Neuroscience	SPM5	39	-	YES	YES	-	-
68	Summerfield and Koechlin, 2010	Frontiers in Neuroscience	SPM2	21	YES	-	YES	-	-
69	Suzuki *et al.*, 2012	Neuron	BVQX	36	-	YES	YES	-	-
70	Symmonds *et al.*, 2010	Journal of Neuroscience	SPM5	16	-	YES	YES	-	-
71	Tanaka *et al.*, 2004	Nature Neuroscience	SPM99	20	-	YES	YES	-	-
72	Tobler *et al.*, 2007	Journal of Neurophysiology	SPM2	16	-	YES	YES	-	-
73	Tom *et al.*, 2007	Science	FSL	16	-	YES	YES	-	-
74	Walter *et al.*, 2008	Neuroimage	SPM2	21	YES	-	-	-	YES
75	Wimmer *et al.*, 2012	European Journal of Neuroscience	SPM5	15	-	YES	YES	-	-
76	Winston *et al.*, 2007	Neuropsychologia	SPM2	26	YES	-	-	-	YES
77	Wu *et al.*, 2011	Journal of Neuroscience	FSL	15	-	YES	YES	-	-
78	Wunderlich *et al.*, 2009	Proceedings of the National Academy of Sciences, *USA*	SPM5	23	-	YES	YES	-	-
79	Wunderlich *et al.*, 2010	Proceedings of the National Academy of Sciences, *USA*	SPM5	24	-	YES	YES	-	-
80	Wunderlich *et al.*, 2012	Nature Neuroscience	SPM8	20	-	YES	YES	-	-
81	Xue *et al.*, 2009	Cerebral Cortex	FSL	13	YES	-	YES	-	-

The studies were identified using PubMed searches and review articles. The CBMA in this study included 81 different fMRI studies and 104 total contrasts. Other information [such as number of subjects (*N*), analysis package used, journal and year of publication) is also included. See 'Methods' section for details.

Table 2 Statistical images included in IBMA

Number	Study	*N*	Reward	Non-zero Voxels	Max *z*	Min *z*
1	Chib *et al.* (2009)	19	Money	54 244	4.75	−3.97
2	Chib *et al.* (2009)	19	Trinkets	54 244	4.63	−4.20
3	Chib *et al.* (2009)	19	Foods	54 244	4.06	−3.06
4	Hare *et al.* (2008)	16	Foods	56 819	5.17	−3.67
5	Hare *et al.* (2009)	37	Foods	51 933	3.54	−3.50
6	Hare *et al.* (2010)	22	Charities	42 606	3.95	−4.22
7	Hare *et al.* (2011a)	33	Foods	81 761	3.75	−3.51
8	Hare *et al.* (2011b)	19	Juices	70 192	5.10	−2.51
9	Hutcherson *et al.* (2012)	25	Foods	97 146	4.83	−4.27
10	Janowski *et al.*, (2013)	32	Movies (Other)	48 256	4.49	−3.28
11	Janowski (2013)	32	Movies (Self)	48 256	7.44	−6.22
12	Kang *et al.* (2011)	24	Trinkets (Hyp)	40 994	4.17	−3.27
13	Kang *et al.* (2011)	24	Trinkets (Real)	40 994	4.97	−3.14
14	Lim *et al.* (2011)	20	Foods	112 677	4.09	−3.65
15	Lin *et al.*, (2012)	22	Money	42 915	4.53	−3.65
16	Lin *et al.*, (2012)	22	Sounds	42 915	3.70	−3.78
17	Litt *et al.*, (2011)	20	Foods	57 475	4.58	−3.21
18	Plassmann *et al.* (2007)	19	Foods	33 971	4.59	−3.73
19	Plassmann *et al.* (2010)	19	Foods	40 975	4.21	−2.75
20	Sokol-Hessner *et al.* (2012)	22	Foods	91 763	4.73	−3.16
21	Wunderlich (2010)	24	Money	56 401	3.82	−4.52

The IBMA in this study included 21 different contrasts from 16 different fMRI studies, all with AR as an author. See 'Methods' section for details.

converted the images to *z*-statistics. To minimize interpolation, all of the images were resampled to a common space using a $3 \times 3 \times 3$ MNI template, which was the voxel size in most of the included studies.

Statistical inference for image-based meta-analysis

We carried out two different tests using IBMA. The first one is based on Stouffer's *z*-statistic, which allows for fixed-effects tests (Lazar *et al.*, 2002; Salimi-Khorshidi *et al.*, 2009). If there are N studies and each study i has a *z*-statistic Z_i at a given voxel, the Stouffer's Z for that voxel across the N studies is equal to: $\sum_i Z_i/\sqrt{N}$. Second, we carried out a random-effects version of the *Z*-maps on the corpus of studies using an ordinary least squares mixed-effects model, implemented in FSL. The statistics reported below are based on the random-effects analysis, although the same set of regions were identified in both cases.

We evaluated the significance of the IBMA using the standard familywise error correction implemented in FSL (Woolrich *et al.*, 2009). Significant voxels were required to have $P < 0.001$ (equivalent to $\sim z > 3.1$) and a cluster forming threshold of $P < 0.05$ was then used across the whole brain. Importantly, as there were differences in brain coverage across studies, using a conservative 'meta-analysis mask' that requires a voxel to be present in all contrasts to be included, would eliminate many of the voxels found in many of the studies, particularly in the parietal lobes. So, we instead employed a more liberal threshold for inclusion in the inference (voxel present in $N > 10$ studies). Note that although this is a more liberal inclusion criterion, it ultimately leads to more conservative significance testing; it increases the number of voxels and thus effectively increases the threshold of the multiple comparisons correction.

As in the CBMA, all coordinates reported here are in MNI space. All images of statistical brain maps were generated using MRICron (Rorden *et al.*, 2007) and the MNI-152 1 mm template.

RESULTS

Regions that reliably correlate with the value of stimuli

We first carried out a CBMA to identify all of the areas that exhibit reliable correlation with behavioral measures of the value of stimuli, both at the time of decision or at the time of outcome, across all tasks and reward modalities. For this reason, the analysis included any foci that were reported to correlate with any parametric measure related to the value of the stimuli, such as decision values, outcome values or chosen values (contrasts = 104, foci = 811). However, it did not include foci in which activity was correlated with variables that are correlated with value, but are not value signals *per se*, such as reward prediction errors.

The CBMA found distinct clusters of VMPFC, ventral striatum (VSTR) and posterior cingulate cortex (PCC) were significantly correlated with this broad measure of subjective value across studies (Figure 1 and Table 3). The VMPFC cluster extends into medial orbitofrontal cortex (OFC) as well as to more anterior parts of PFC, such as frontopolar cortex and anterior MPFC. It includes both regions of subgenual and subcallosal anterior cingulate cortex (ACC) (Beckmann *et al.*, 2009) and lies within networks commonly referred

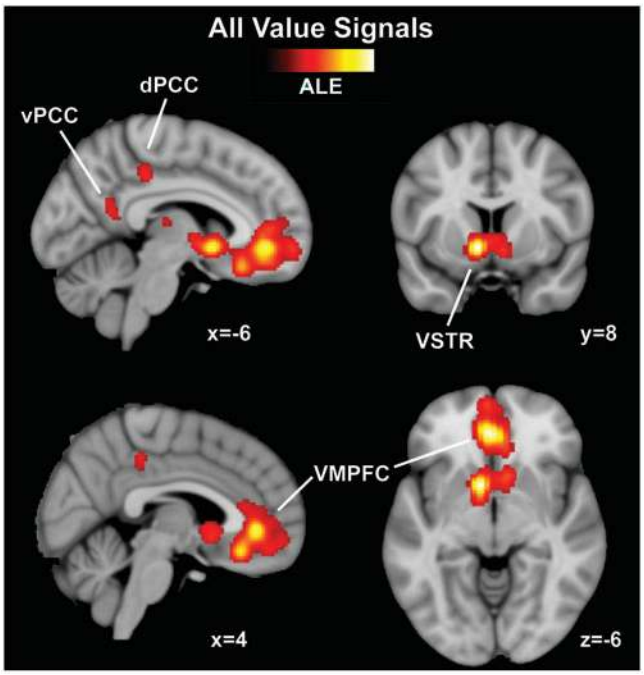

Fig. 1 Reliable neural features of value identified using CBMA. To first identify all brain regions that reliably contain any value-related information, we used all available contrasts of subjective value ($N = 104$). We found distinct clusters in VMPFC, VSTR and both dorsal and ventral PCC. The VMPFC cluster also extended into subgenual cingulate as well as regions commonly labeled medial prefrontal cortex and frontal polar cortex. The global maximum ALE value (ALE $= 68.89 \times 10^{-3}$) was located in left VSTR. The scale reflects ALE values determined to survive a voxel-level significance of $P < 0.001$ and a cluster-corrected threshold of $P < 0.05$. The colorbar spans ALE values of 18.23×10^{-3} (min) to 68.89×10^{-3} (max). Coordinates and cluster information are listed in Table 3.

Table 3 Maxima and cluster information for CBMA of all parametric subjective value contrasts in the dataset

Cluster	Volume (mm^3)	ALE ($\times 10^{-3}$)	x	y	z	Region
1	26 088	68.89	−8	8	−6	Left nucleus accumbens (VSTR)
-	-	67.88	−2	40	−4	Anterior cingulate cortex (VMPFC)
-	-	53.26	−2	28	−18	Subcallosal cortex (VMPFC)
-	-	35.47	10	14	−4	Right nucleus accumbens (VSTR)
-	-	33.18	−4	58	−8	Frontal polar cortex (VMPFC)
2	1600	42.65	−2	−34	42	Dorsal posterior cingulate cortex
3	640	26.81	−8	−56	20	Ventral posterior cingulate cortex
4	464	29.37	−22	34	−16	Left orbitofrontal cortex
5	272	24.48	−8	−20	10	Left thalamus

The CBMA of subjective value (contrasts = 104, foci = 811) identified five distinct clusters using ALE. Results are displayed in Figure 1.

to as the orbital-prefrontal and medial-prefrontal networks (Price and Drevets, 2010). For PCC, there were two distinct clusters, ventral (vPCC) and dorsal (dPCC). An additional cluster was also found in the thalamus, centered on a subregion of the thalamus previously shown to have strong projections to prefrontal cortex (Behrens *et al.*, 2003). The cluster containing the global maximum ALE statistic was found in left VSTR (ALE $= 68.89 \times 10^{-3}$).

The CBMA results in Table 3 and Figure 1 suggest that there might be a left–right asymmetry for the probability that ventral prefrontal cortex reflects the computation of subjective value. Given the importance of this region in the decision-making literature, we carried out an additional *post hoc* test: we used four anatomical ROIs from the Automatic Anatomical Labeling (AAL) atlas to test whether higher ALE values were more likely in the left as opposed to right ventral prefrontal cortex. We also selected two coordinates from the Harvard-Oxford atlas [(x,y,z) = (±22,24,−22) and (x,y,z) = (±32,36,−14)]. The probabilistic atlas assigns >90% to OFC for the first set of coordinates and approximately splits OFC and frontal polar cortex with the second set of coordinates. We drew 6 mm radius spheres about these coordinates in each hemisphere. After generating a null distribution from 10 000 permutations of ALE values across the two hemispheres for each ROI, we compared the difference in average ALE values for several subregions of ventral prefrontal cortex (Table 4). Looking at the four different AAL structures, the left mask exhibited a significantly greater average ALE ($P < 0.001$) in three of the four masks, with only the orbital part of the inferior frontal gyrus in the opposite direction). The average ALE statistic was also larger on the left when the four masks were combined ($P < 0.001$). The same was also true for the spherical OFC region (±22,24,−22). We also looked at the total number of voxels in the left hemisphere that were greater than the maximum ALE value in the right hemisphere (right-most column in Table 4). This measure also supports a trend for greater ALE statistics in the left hemisphere. So, at least for our corpus of studies, there appears to be an increased likelihood for peak coordinates associated with the computation of subjective values to be reported in left ventral prefrontal cortex.

The amygdala, an additional area often associated with the computation of value (Rolls, 2000; Seymour and Dolan, 2008), did not survive our statistical threshold. However, a small cluster in left amygdala did pass a voxel-level threshold of $P < 0.005$ (without cluster correction).

Distinct subnetworks co-activate with the VMPFC stimulus value regions

We next investigated how the set of areas that exhibit reliable correlation with stimulus value signals is organized into distinct subnetworks that co-activate together. In particular, as our meta-analysis of all possible stimulus value measures identified three local clusters in VMPFC (Figure 1 and Table 3), we hypothesized that those subregions of VMPFC might be part of distinct subnetworks involved in the computation of various value-related signals. To test this hypothesis, we constructed three spherical 9 mm ROIs around the coordinates exhibiting local maxima in the previous ALE analysis (Figure 2a). We refer to these ROIs as central VMPFC [cVMPFC, red; (x,y,z) = (−2,40,−4)], ventral VMPFC [vVMPFC, blue; (x,y,z) = (−2,28,−18)] and anterior VMPFC [aVMPFC, green; (x,y,z) = (−4,58,−8)]. Then, we looked for areas that exhibited reliable co-activation across the corpus of studies. Of these three ROIs, cVMPFC was the one for which the most significant correlation with stimulus values was reported in the previous literature (contrasts = 19, foci = 200), followed by vVMPFC (contrasts = 17, foci = 120) and aVMPFC (contrasts = 9, foci = 105).

The analysis revealed common and distinct areas of co-activation with the three VMPFC ROIs. All of the significant common regions of co-activation were constrained to the subgenual portion of the cingulate cortex and generally within the cVMPFC seed (Figure 2b). Two of the three ROIs also exhibited co-activation with distinct cortical networks (Figure 2c). The first seed region, cVMPFC, significantly co-activated with dPCC (ALE $= 26.32 \times 10^{-3}$), left VSTR (ALE $= 21.86 \times 10^{-3}$), lateral OFC (lOFC, ALE $= 15.10 \times 10^{-3}$) and SFG (ALE $= 14.71 \times 10^{-3}$). In contrast, aVMPFC reliably co-activated with left angular gyrus (ANG) near the temporal parietal junction (ALE $= 13.38 \times 10^{-3}$) and vPCC (ALE $= 13.57 \times 10^{-3}$). Although the ANG result for aVMPFC does survive in a direct contrast of ALE maps

with cVMPFC ($P < 0.005$), the other pairwise comparisons do not survive a direct contrast, even at lower thresholds. A potential reason is that these other pairwise comparisons of ALE maps are relatively underpowered (e.g. 9 and 17 contrasts), a limitation that should be addressed in future meta-analyses that can rely on a larger sample of studies. Interestingly, the regions co-activating with the cVMPFC and aVMPFC seeds are remarkably similar to some of the subnetworks of the canonical default mode network, a result found across a wide variety of tasks (Smith *et al.*, 2009; Andrews-Hanna *et al.*, 2010).

Comparison of decision and outcome value signals

We next tested if distinct sets of areas are involved in the computation of stimulus values at the time of decision and at the time of outcome (Rangel and Hare, 2010; Rushworth *et al.*, 2011). To look for reliable commonalities or differences in decision and outcome value computations, the test was carried out in several steps.

Table 4 Lateralization tests for ventral prefrontal cortex results in CBMA

ROI	Ave ALE L	StDev ALE L	Ave ALE R	StDev ALE R	Ave ALE L-R	*P*-value	*Total L > R Max*
OFC	8.48	10.11	6.26	8.31	2.22	$P < 0.001$	5
Med OFC	25.03	12.55	18.05	11.41	6.98	$P < 0.001$	5
Mid OFC	6.26	5.6	0.79	1.24	5.47	$P < 0.001$	175
Inf OFC	3.66	3.95	5.78	4.39	−2.11	$P < 0.001$	10
Sup OFC	6.63	4.99	2.5	2.57	4.12	$P < 0.001$	146
(±22,24,−22)	7.07	5.48	1.83	1.8	5.24	$P < 0.001$	91
(±32,36,−14)	4.45	4.98	5.57	3.58	−1.12	$P < 0.002$	18

A *post hoc* analysis of ALE estimates in the CBMA reported in Figure 1 identified several significant differences between several regions of ventral prefrontal cortex. ROIs were defined using AAL structures: the orbital parts of the inferior frontal gyrus (Inf Orb), superior frontal gyrus (Sup Orb), middle frontal gyrus (Mid Orb) and the more medial-orbital portion of the superior frontal gyrus (Med Orb). See 'Results' section for details.

First, we completed a CBMA to look for areas that exhibit reliable correlations with stimulus value at the time of decision. So, this analysis was constrained to the subset of studies and contrasts that looked at parametric measures of subjective value during the decision phase (contrasts = 69, foci = 571). This analysis identified a network of regions that included a large cluster in VMPFC extending to frontal polar cortex and MPFC and smaller clusters in bilateral VSTR and dPCC (Figure 3 and Table 5). The global maximum ALE statistic was found in the paracingulate gyrus, part of the VMPFC cluster ($ALE = 63.29 \times 10^{-3}$).

Second, we were able to carry out a parallel IBMA of decision value, which is the gold standard test for reliability in fMRI meta-analysis studies (Salimi-Khorshidi *et al.*, 2009; Kober and Wager, 2010). The IBMA identified a similar set of regions demonstrating a positive correlation with value (Figure 4 and Table 6), including VMPFC, which was the global maximum [(x,y,z) = (0, 39,−3), maximum $z = 6.88$]. The IBMA also found distinct clusters of activation in dPCC and vPCC, paralleling the results found in the CBMA (Figure 1) for the pooled value signals. An additional cluster was also identified in the superior frontal gyrus (SFG).

Our IBMA also afforded us the opportunity to inspect the data for negative correlates of decision value, an option that was not possible in the CBMA as most studies do not report negative correlations with subjective value. We found no voxels that survived the threshold employed for the main IBMA result. However, two loci survived a lower threshold of $P < 0.005$ (no cluster-level correction) and we report them for completeness: precentral gyrus [(x,y,z) = (−60,9,12), $z = 3.29$, 4 voxels) and SFG [(x,y,z) = (18,0,72), $z = 2.89$, 2 voxels].

Two differences between the IBMA and CBMA results regarding the computation of value at the time of decision are noteworthy: the

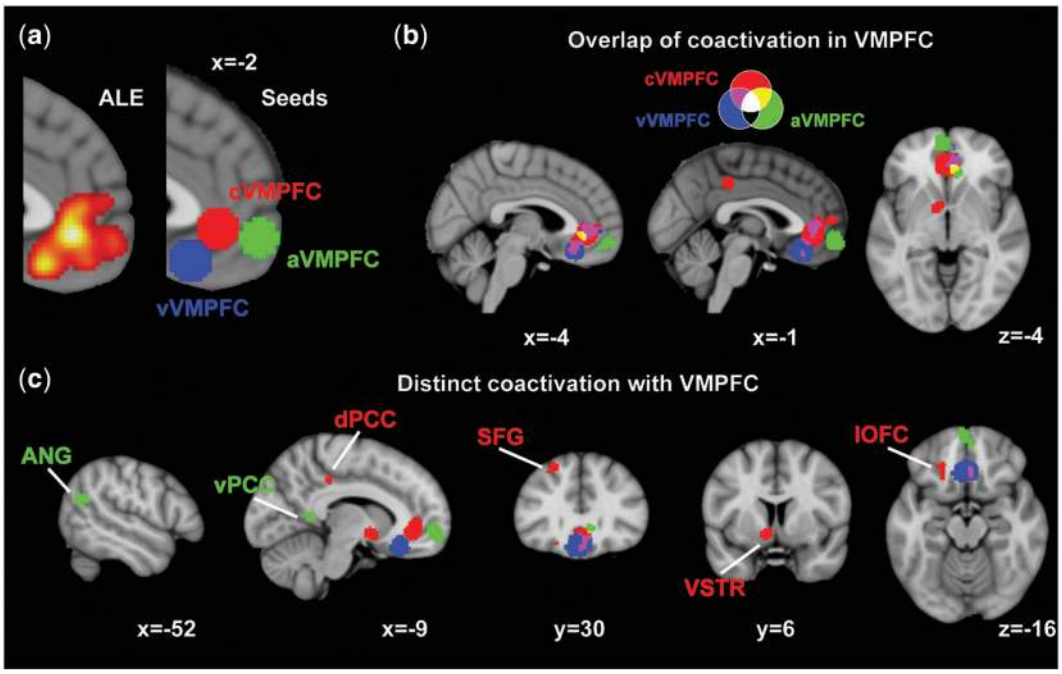

Fig. 2 Common co-activation with VMPFC during value computation. (**a**) Three local maxima were identified in the large ventral PFC cluster in the ALE analysis that included all values (left, from Figure 1). The global maximum was located in central VMPFC (cVMPFC, red), and two distinct local maxima were more anterior (aVMPFC, green) and ventral (vVMPFC, blue) to the global maximum. Around each of those three coordinates, a 9 mm radius sphere was drawn (right) to identify contrasts with reported foci in the vicinity of those local maxima. (**b**) Several common areas in VMPFC were found to be active across all three seed regions (white). The same cluster threshold for significance in all other ALE tests was applied here. (**c**) Both the cVMPFC seed and the aVMPFC seed had several distinct areas of co-activation. For cVMPFC (red), this included dPCC, SFG, VSTR and lOFC. For aVMPFC (green), this included ANG) as well as vPCC.

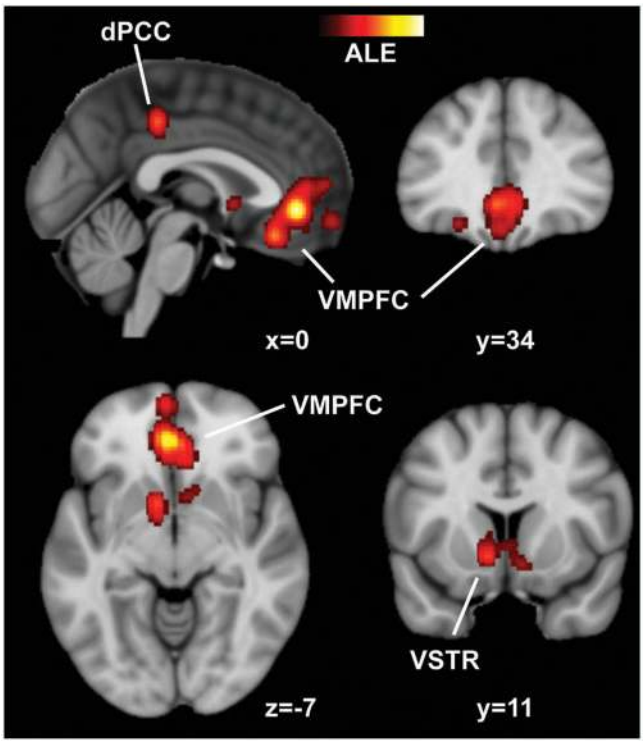

Fig. 3 Reliable neural features of value during the decision phase using CBMA. We collected all available contrasts for value signals during a decision phase ($N = 69$) to identify consistent positive correlations with decision value signals. The global maximum (ALE $= 63.29 \times 10^{-3}$) was found in VMPFC, and consistent activation was also found in dPCC and VSTR. Notably, the VMPFC cluster extended to other parts of the ventral and anterior parts of prefrontal cortex. The scale reflects ALE values determined to survive a voxel-level significance of $P < 0.001$ and a cluster-corrected threshold of $P < 0.05$. The colorbar spans ALE values of 15.70×10^{-3} (min) to 63.29×10^{-3} (max). Coordinates and cluster information are listed in Table 5.

Table 5 Maxima and cluster information for CBMA of decision values

Cluster	Volume (mm^3)	ALE ($\times 10^{-3}$)	x	y	z	Region
1	15 312	63.29	−2	40	−6	Paracingulate gyrus (VMPFC)
-	-	40.94	4	30	−16	Subcallosal cortex (VMPFC)
-	-	29.48	−4	60	−10	Frontal polar cortex (VMPFC)
2	3536	39.70	−10	8	−6	Left nucleus accumbens (VSTR)
-	-	22.51	10	12	−10	Right nucleus accumbens (VSTR)
3	1688	36.91	0	−34	42	Dorsal posterior cingulate cortex
4	440	24.29	−24	32	−16	Left orbitofrontal cortex

The CBMA of decision value (contrasts = 69, foci = 571) identified four distinct clusters using ALE. Results are displayed in Figure 3.

cluster of significant activity in VSTR appears more robust in the CBMA than in the IBMA and the SFG exhibiting reliable correlation with stimulus values at the time of decision in the IBMA, but not in the CBMA. The difference in SFG significance is perhaps attributable to the influences of subthreshold results that are only obtainable in IBMA (Salimi-Khorshidi *et al.*, 2009). With respect to the differences in VSTR, as all of the IBMA studies come from the same laboratory, one natural explanation would be that the fMRI data acquisition used by this group has a limited ability to identify signal in the VSTR. However, several of the included papers have reliably found activity in this area related to value and prediction errors (Hare *et al.*, 2008; Lim *et al.*, 2011; Litt *et al.*, 2011). As many of the IBMA studies used food as the reward modality, another potential explanation is that somehow food has a differential ability to activate the VSTR in response to value. Again, this seems unlikely, as several of the studies cited above reliably exhibit value activity in this area in tasks involving foods. Understanding why the VSTR correlates with subjective values in some paradigms but not in others is a critical question for future research.

Third, we carried out a CBMA to look for areas that exhibit reliable correlations with stimulus value at the time of outcome across studies. Note that a value measure at the time of reward receipt (e.g. delivery of reward such as juice or a visual image) is computationally distinct from a stimulus value computed for the purpose of guiding decisions. For this analysis we only included the subset of studies and contrasts that looked at parametric measures of subjective value during the outcome or reward consumption phase (contrasts = 32, foci = 200). The analysis identified two distinct clusters (Figure 5 and Table 7): one in VMPFC/OFC (ALE $= 20.20 \times 10^{-3}$) and one in bilateral VSTR (ALE $= 21.98 \times 10^{-3}$).

Finally, we carried out a direct contrast of the ALE maps associated with the computation of stimulus values at decision and outcome, in order to identify regions that are more reliably associated with one of these phases across studies (Figure 6 and Table 8). The results in both directions of the contrast were very focal. Both dPCC and a specific subregion of VMPFC were more reliably correlated with decision values than with outcome values (Figure 6a). In contrast, a more anterior part of MPFC (near the frontal pole) and a portion of subcallosal cortex (very near VSTR) were more reliably correlated with outcome values (Figure 6b). We also performed a conjunction analysis of the ALE maps for decision value and outcome value (Figure 6c). This analysis revealed that VSTR and a region of VMPFC (more medial than the one depicted in Figure 6b) were reliably associated with both value computations.

Value signals for different reward modalities

Finally, we carried out a CBMA to investigate if there is evidence for regional specialization in the computations of stimulus values for different reward modalities (e.g. food *vs* money). To investigate this question, we took the corpus of reported results and partitioned it by reward modality, while making no distinction between the timing of the value signal (i.e. decision *vs* outcome). Of the possible categories, the most common reward modality was money (contrasts = 50, foci = 432). We also had a large number of studies using various types of foods (e.g. snack foods or juices; contrasts = 24 contrasts, foci = 163). Finally, we had a remaining set of studies with other rewards (e.g. rewarding visual images such as human faces, or donations to charities; contrasts = 24 contrasts, foci = 143). The handful of studies that employed multiple reward modalities on a single trial was excluded from this analysis.

Each of the three sets of studies revealed several reliable clusters of activation (Figure 7). The global maximum for money (ALE $= 43.57 \times 10^{-3}$) was in VMPFC, but there were also distinct clusters in VSTR, dPCC and SFG (Figure 7a). For food, the global maximum (ALE $= 26.21 \times 10^{-3}$) was also in VMPFC, but with a more posterior peak (Figure 7b). For the other category, the maximum (ALE $= 32.88 \times 10^{-3}$) was located in VSTR, but there was also a separate cluster in VMPFC (Figure 7c). Note that for money, the larger extent of the ALE maps is due, most likely, to the fact that there is more data reported for that modality and thus our analyses have more statistical power in that case. Additional cluster information for each reward modality is listed in Table 9.

To identify areas that were significant with value across all the reward modalities, we took the intersection of money, food and other maps (Figure 7d, left). Only a portion of VMPFC was significant

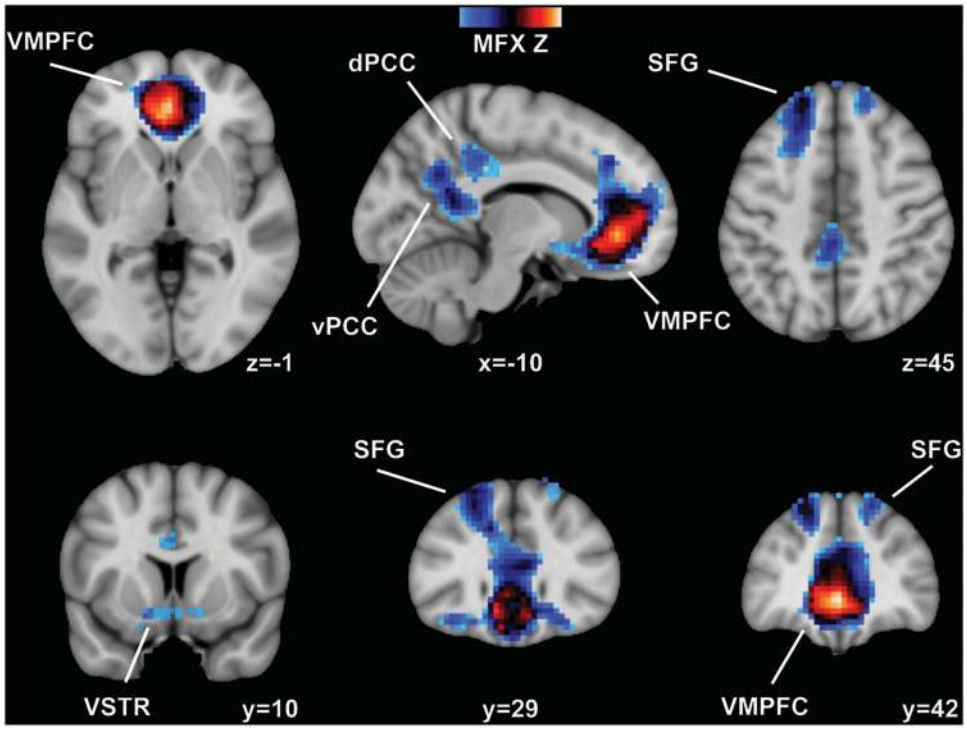

Fig. 4 Reliable neural features of value during the decision phase using IBMA. We used data from previously published studies ($N = 21$ contrasts). We performed a mixed-effects analysis to identify consistently positive correlation with measures of stimulus or decision value. The IBMA identified distinct clusters in VMPFC, dPCC and vPCC as well as SFG. The VMPFC cluster extended into the ventral part of the striatum (VSTR). The global maximum ($z = 6.88$) was located in VMPFC. The scale reflects mixed-effects z-scores determined to survive a voxel-level significance of $P < 0.001$ and a cluster-corrected threshold of $P < 0.05$. The colorbar spans z-values of 3.10 (min) to 6.88 (max). Coordinates and cluster information are listed in Table 6.

Table 6 Maxima and cluster information for IBMA of decision values

MFX-Z	x	y	z	Region
6.88	0	39	−3	VMPFC
5.16	−18	42	45	SFG
5.13	−6	−51	15	vPCC
4.46	−3	−21	39	dPCC

We performed a mixed-effects analysis on statistical maps from 21 different decision value contrasts listed in Table 2. Results are displayed in Figure 4.

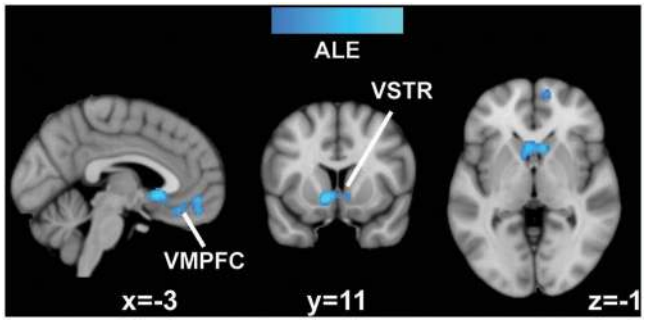

Fig. 5 Reliable neural features of value during the outcome phase using CBMA. Using all available outcome value contrasts ($N = 32$), we identified several significant clusters of consistent outcome value across studies in VMPFC and VSTR. The global maximum (ALE $= 21.98 \times 10^{-3}$) was located in left VSTR. The scale reflects ALE values determined to survive a voxel-level significance of $P < 0.001$ and a cluster-corrected threshold of $P < 0.05$. The colorbar spans ALE values of 10.54×10^{-3} (min) to 21.98×10^{-3} (max). Coordinates and cluster information are listed in Table 7.

in all three. We also inspected the ALE maximum in VMPFC for each of the reward categories (Figure 7d, right), using coordinates surrounded by 5 mm radius spheres for display purposes. The most ventral and posterior maximum clearly belongs to studies of food. Although one of the money local maxima (green) overlaps with the other category (blue), we note that the reward modality with the most anterior cluster was money. This result also holds if the other category is split into rewards that are immediately consumable (e.g. visual images) and the remaining unclassified reward types (cyan for 'consumable' and magenta for 'miscellaneous', Figure 7d, far right). This gradient suggests a posterior-to-anterior gradient of value representations for reward modalities, with posterior corresponding to more concrete rewards and anterior to more abstract rewards. Importantly, we also performed a direct test across these reward modalities. Although the contrasts have limited statistical power, a direct contrast of money and food found a significantly greater likelihood for food in posterior VMPFC [$P < 0.005$, maximum z located at $(x,y,z) = (-8,27,-13)$] and for money in anterior VMPFC [$P < 0.005$, $(x,y,z) = (-5,60,-9)$]. Similarly, a contrast of other relative to money found a significantly greater activation likelihood near the peak for other in Figure 7d [$P < 0.005$, $(x,y,z) = (-12,46,11)$] and a more dorsal anterior part of MPFC [$P < 0.005$, $(x,y,z) = (-1, 56,10)$] for money relative to other. The third pair of comparisons, between food and other, had the least power, but again found a posterior portion of VMPFC for food relative to other ($P < 0.005$, $(x,y,z) = (-4,28,-20)$]. The opposite contrast, however, did not find any significant differences, even at the more liberal threshold of $P < 0.01$.

One important concern with this last set of analyses is that, across studies, there might be a substantial correlation between the type of reward and the time of the value signal. For example, while studies of

value coding at the time of consumption frequently use liquids and foods (e.g. receiving a squirt of juice in the scanner), studies using trinkets or money as rewards can effectively only look at value coding at the time of decision (e.g. choosing between two gambles). To address this concern, we carried out one additional *post hoc* test in which we fixed the reward modality to foods, and computed separate ALE values at the time of decision and at the time of outcome (Figure 8). Unfortunately, due to the smaller number of studies available (12 for each decision and outcome), the tests are comparatively underpowered. For that reason, we report all results at $P < 0.001$, without a cluster-level correction. As can be seen in Figure 8, the results are similar to those for the comparison between decision and outcome value signals, including the robust posterior VMPFC result for food.

DISCUSSION

We have carried out a comprehensive meta-analysis of fMRI studies that use computational methods to study value-based choice. The large number of studies included allowed us to investigate four basic questions that cannot easily be addressed within a single fMRI study. We organize our discussion around the key findings relating to these questions.

First, we characterized the full set of areas that reliably correlate with stimulus values when they need to be computed (i.e. either at the time of decision or at the time of outcome) across tasks and reward modalities. We found that neural responses in VMPFC and VSTR are correlated with various measures of stimulus values across a wide range of decision tasks, reward modalities and stages of the decision-making process. This result is consistent with recent reviews of the literature (Rangel *et al.*, 2008; Wallis and Kennerley, 2010; Glimcher, 2011; Grabenhorst and Rolls 2011; Padoa-Schioppa, 2011; Rushworth *et al.*, 2011), although the meta-analysis used here provides a more rigorous test of the reliability of these findings across studies.

Unlike VMPFC and VSTR, however, PCC is an area that has received much less attention in the value-based choice literature. Yet, our results establish the reliability of activity correlated with stimulus values in two distinct loci in PCC, a ventral region and a more dorsal region. Indeed, distinct clusters are apparent in both the CBMA

Table 7 Maxima and cluster information for CBMA of outcome values

Cluster	Volume (mm^3)	ALE ($\times 10^{-3}$)	x	y	z	Region
1	4744	20.20	0	32	−18	Frontal medial cortex (VMPFC)
-	-	17.75	8	46	−12	Frontal medial cortex (VMPFC)
-	-	14.73	10	60	0	Frontal polar cortex
-	-	12.73	−10	30	−18	Orbitofrontal cortex
2	2912	21.98	−8	10	−6	Left nucleus accumbens (VSTR)
-	-	19.24	8	14	−4	Right nucleus accumbens (VSTR)

The CBMA here (contrasts = 32, foci = 200) identified four distinct clusters using ALE. Results are displayed in Figure 5.

Table 8 CBMA comparison of decision and outcome values.

Cluster	Volume (mm^3)	Max *z*	x	y	z	Region
Decision > Outcome						
1	536	3.06	0	−30	40	Dorsal posterior cingulate cortex
2	344	3.19	−8	36	0	Anterior cingulate gyrus (VMPFC)
3	16	2.71	−4	50	2	Paracingulate gyrus/frontal pole
4	16	2.77	−52	32	4	Inferior frontal gyrus
5	16	2.74	−2	58	12	Frontal pole frontal medial cortex
Outcome > Decision						
1	232	3.12	18	56	−6	Frontal pole (MPFC)
2	200	2.99	−2	20	−4	Subcallosal cortex

Differences in ALE values for decision and outcome were contrasted and converted to *z*-scores. Results are displayed in Figure 6.

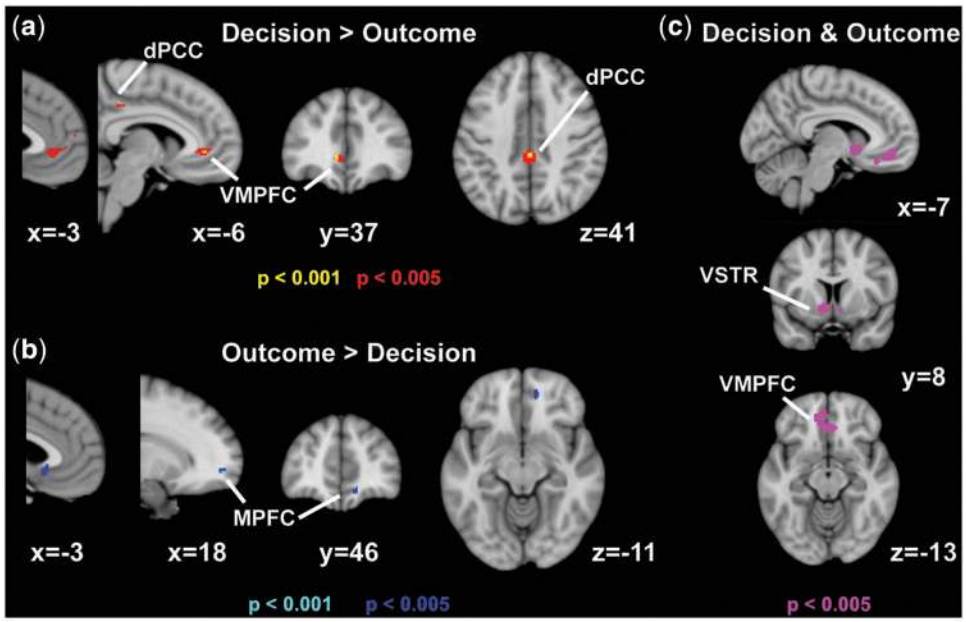

Fig. 6 Comparison of decision and outcome value signals using CBMA. To determine if different brain regions are differentially recruited during the decision and outcome phase, we contrasted ALE images for the decision and outcome phase. (**a**) The decision > outcome comparison identified significant differences in both dPCC and VMPFC near subgenual cingulate. (**b**) The outcome > decision contrast identified a more anterior area of MPFC, as well as subcallosal cortex. (**c**) A conjunction of the two value computations, using the ALE maps presented in Figures 3 and 5, revealed common activation in VSTR and another portion of VMPFC. Coordinates and cluster information for the contrasts are listed in Table 8.

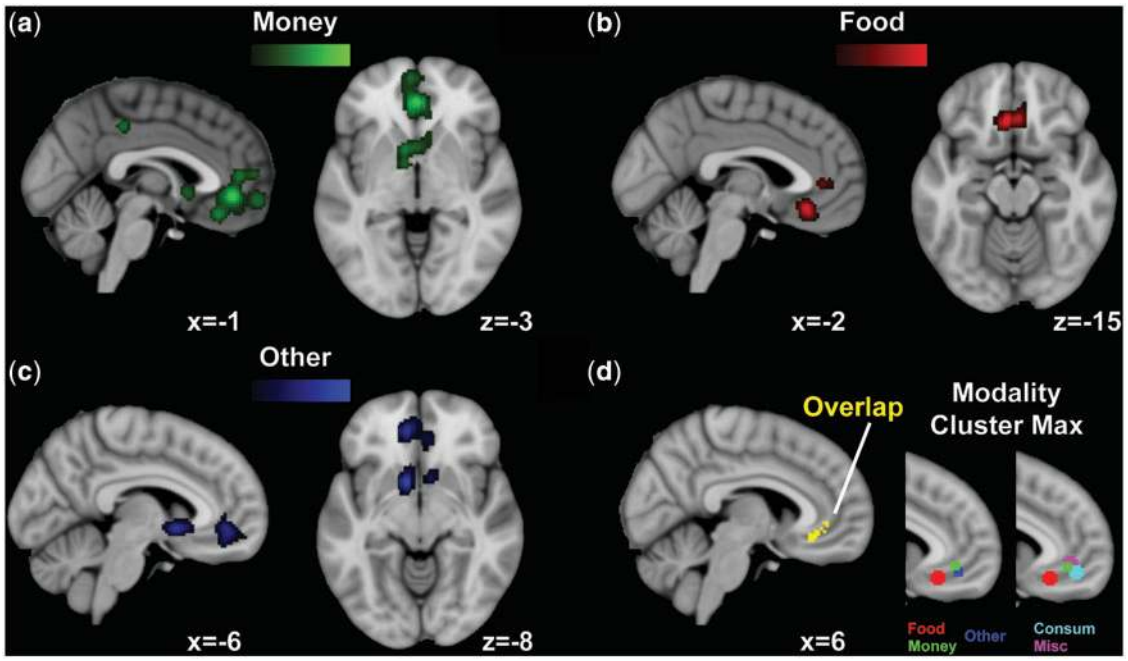

Fig. 7 Comparison of value in different reward modalities using CBMA. (**a**) Using all value contrasts involving money as a reward modality ($N = 50$), we found significant ALE values in VMPFC, VSTR and dPCC. The colorbar spans ALE values of 13.95×10^{-3} (min) to 43.57×10^{-3} (max). (**b**) We performed the same analysis for studies using food as rewards ($N = 24$). This analysis revealed only two significant clusters, in a more ventral and posterior portion of VMPFC. The colorbar spans ALE values of 9.81×10^{-3} (min) to 26.21×10^{-3} (max). (**c**) Using 'other' to collect all other value contrasts using a single reward modality ($N = 24$), we again found reliable VMPFC and VSTR activity. The colorbar spans ALE values of 9.70×10^{-3} (min) to 32.88×10^{-3} (max). (**d**) Here, on the right, the cluster maxima coordinates are surrounded by 5 mm radius spheres for display. We see that most ventral maximum belongs to studies of food. Although one of the money local maxima (green) overlaps with the other category (blue), we note that the only reward modality with the most anterior cluster was money. This represents a posterior-to-anterior representation of reward modalities. The scales in (a)–(c) reflect ALE values determined to survive a voxel-level significance of $P < 0.001$ and a cluster-corrected threshold of $P < 0.05$. Coordinates and cluster information are listed in Table 9.

Table 9 Comparison of reward modalities using CBMA

Cluster	Volume (mm^3)	ALE ($\times 10^{-3}$)	x	y	z	Region
Money	($N = 50$)					
1	9960	43.57	−2	40	−6	Paracingulate gyrus (VMPFC)
-	-	28.38	2	32	−18	Frontal medial cortex
-	-	24.31	0	58	−8	Frontal polar cortex
2	3528	28.44	−8	8	−6	Left nucleus accumbens (VSTR)
-	-	17.06	8	18	−4	Right nucleus accumbens (VSTR)
-	-	15.80	−8	12	6	Left caudate
3	760	26.98	−2	−34	42	Dorsal posterior cingulate cortex
4	480	18.39	−24	30	50	Superior frontal gyrus
Food	($N = 24$)					
1	3504	26.21	−4	28	−14	Subcallosal cortex (VMPFC)
2	1512	16.18	−2	40	2	Cingulate gyrus
-	-	15.12	8	44	0	Paracingulate gyrus
Other	($N = 24$)					
1	4760	25.39	−10	42	−10	Frontal medial cortex (VMPFC)
-	-	16.83	4	38	−6	Anterior cingulate gyrus
-	-	13.04	6	48	−14	Frontal medial cortex
-	-	10.21	−4	62	−14	Frontal polar cortex
2	2288	32.88	−8	8	−6	Left nucleus accumbens (VSTR)
3	728	16.54	10	14	−6	Right nucleus accumbens (VSTR)
4	480	15.35	14	−20	4	Right thalamus

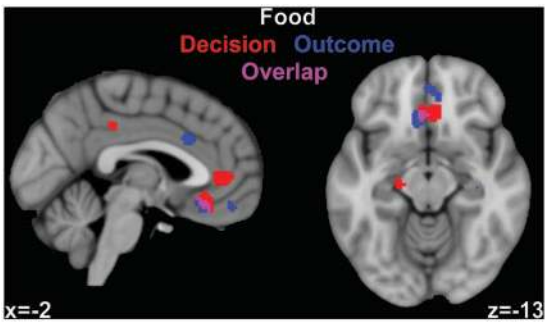

Fig. 8 Decision and outcome values of food studies using CBMA. The ALE analyses here reflect a *post hoc* test of the studies involving only food ($N = 24$), with decision value (red) and outcome value (blue) calculated separately. As would be expected, overlap occurs in the same posterior VMPFC area highlighted in Figure 7. All voxels shown survive voxel-level significance of $P < 0.001$.

(Figure 1) and IBMA (Figure 4) results. These two regions of PCC have been implicated in various functions that might be useful in guiding the computation of values, such as attending to internal *vs* external influences (Nakao *et al.*, 2012), remembering past events or envisioning future ones (Schacter *et al.*, 2007) and monitoring local environment changes (Pearson *et al.*, 2011). PCC is also a central node of the default mode network (Buckner *et al.*, 2008), and recent work has made distinctions between ventral and dorsal PCC that may correspond to some of the aforementioned functions (Leech *et al.*, 2011). Understanding the precise role of the PCC in the network of regions that contribute to value-based decisions remains an important and open question.

Another area that deserves further consideration is the superior frontal sulcus (SFS), which demonstrated a significant and reliable correlation with decision value in our IBMA. Although the precise contribution of SFS to value-based choice is unknown, it is worth noting that the reported cluster in our IBMA closely neighbors the coordinates reported to correspond to sensory evidence in a perceptual decision-making task (Heekeren *et al.*, 2004) and includes the SFS

coordinates reported for the comparisons of cost and benefit in a value-based choice task (Basten *et al.,* 2010).

Second, we asked if the set of areas associated with valuation are organized into dissociable functional networks across tasks and reward modalities. We found that a broad region of VMPFC contains a reliable value signal, a fact that has been previously noted (Grabenhorst and Rolls, 2011; Wallis, 2012). However, our co-activation results (Figure 2) suggest that this region of VMPFC is divided into subregions that co-activate with different networks: one that involves central VMPFC, dorsal dPCC and VSTR, and another that involves more anterior VMPFC, left ANG and vPCC. These results corroborate a recent functional parcellation of OFC (Kahnt *et al.,* 2012), which found evidence for the existence of an interaction between distinct functional networks within OFC. Furthermore, these two networks involving VMPFC are remarkably similar to some of the subnetworks of the default mode network found across a wide variety of tasks (Smith *et al.,* 2009; Andrews-Hanna *et al.,* 2010). An intriguing hypothesis is that different value computations require different levels of episodic memory and mental simulations and are thus likely to recruit regions associated with the default mode network (Pearson *et al.,* 2011; Mars *et al.,* 2012). The centrality of VMPFC for integrating this relevant information from a variety of networks has been argued elsewhere (Roy *et al.,* 2012).

Third, we tested for commonalities and dissociations in the set of areas involved in the computation of stimulus values at decision and outcome. Our results suggest a dissociation with respect to the comparison of stimulus value signals at decision and outcome. We found that dorsal PCC and a specific subregion of central VMPFC were more reliably correlated with decision values than with outcome values, whereas a more anterior part of MPFC (near the frontal pole) and a portion of subcallosal cortex (near VSTR) were more reliably correlated with outcome values (Figure 6). However, the most striking pattern was the existence of reliable stimulus value-related activity in regions of VMPFC and VSTR at both decision and outcome. This commonality suggests the interesting possibility that these areas are involved in computing stimulus value whenever such variables are needed, regardless of the phase of the decision task.

Fourth, we investigated for commonalities and dissociations in the set of areas involved in the computation of stimulus values for different reward modalities (e.g. food *vs* money). We found that reward modality may also affect the precise location of VMPFC in which value is encoded. Our results include suggestive evidence of a posterior-to-anterior gradient of value representations (Figure 7), corresponding to concrete-to-abstract rewards. This finding is consistent with previous hypotheses and results (Kringelbach and Rolls, 2004; Sescousse *et al.,* 2010; Grabenhorst and Rolls, 2011), although those primarily discuss OFC. Anatomical studies of OFC connectivity, such as those looking at sensory inputs to OFC, suggest that it might be organized in a graded fashion (Carmichael and Price, 1995). A more recent report, looking specifically at decision value computations (McNamee *et al.,* 2013), also finds evidence for such a gradient. A comprehensive understanding of the extent of such a hierarchy of value representation in OFC and VMPFC, however, will likely require both more cross-species work (Wallis, 2012) and careful analysis of how different fMRI acquisition sequences may affect results in more orbital parts of prefrontal cortex (Roy *et al.,* 2012). Furthermore, our results employ a fairly coarse classification of reward modality. Even within food rewards, it would be a valuable exercise to consider the different sensory contributions to food evaluation (Rolls and Grabenhorst, 2008). An exciting avenue for further work would be to generate cleaner taxonomies of reward modalities and their complexity as well as if and how those might have similar or distinct neural representations along a VMPFC gradient.

Notably, our analyses did not identify several regions commonly associated with decision-making computations. First is the more dorsal region of the ACC and the neighboring dorsal medial prefrontal cortex (DMPFC). This area has had several wide classes of computations attributed to it, including decision and strategic control (Venkatraman *et al.,* 2009), environment volatility (Behrens *et al.,* 2007) and multiplexing of decision parameters (Kennerley *et al.,* 2009; Hayden and Platt, 2010; Hare *et al.,* 2011b). Similarly, action value signals—which take into account the action costs associated with the choice of a particular option—are also commonly attributed to ACC (Rangel and Hare, 2010; O'Doherty, 2011). These distinct computational roles for ACC and DMPFC, coupled with those areas appearing in comparatively few contrasts of interest in fMRI studies of simple choice, are likely reasons for their absence in our results. Second, the amygdala is also commonly discussed in various aspects of reward processing (Rolls, 2000; Gottfried *et al.,* 2003, Seymour and Dolan, 2008). Although a correspondence between subjective value and amygdala was identified at a lower threshold in our CBMA, the precise computations that amygdala contributes to subjective value may not be sufficiently represented in our corpus of studies. Finally, various parts of dorsal lateral prefrontal cortex (DLPFC), which have been found in some studies to correlate with representations of stimulus values (Plassmann *et al.,* 2007; Hare *et al.,* 2009; Plassmann *et al.,* 2010; Baumgartner *et al.,* 2011; Hutcherson *et al.,* 2012), were also not identified in the meta-analyses. One potential explanation for this negative result is that DLPFC might only be involved in tasks involving the evaluation of sufficiently abstract stimuli or self-regulation (Hutcherson *et al.,* 2012), which are relatively uncommon in the existing literature.

There are also some important limitations of the study. First, we were unable to consider contrasts from paradigms that involve the comparison of options from distinctly different reward modalities (e.g. choosing movie tickets *vs* ice cream). Although some fMRI studies do take various approaches to address this issue (FitzGerald *et al.,* 2009; Grabenhorst *et al.,* 2010; Smith *et al.,* 2010; Levy and Glimcher, 2011), there are relatively few of these, so our meta-analyses did not directly assess the reliability of such value computations. As more studies attempt to identify common scales of valuation and comparison of different reward domains, it will be intriguing to test the spatial reliability of areas that demonstrate this property (Grabenhorst *et al.,* 2010, Levy and Glimcher 2011, McNamee *et al.,* 2013). Second, we did not formally test the coding of value for appetitive and aversive stimuli, although clearly a full understanding of value computation is incomplete in their absence (Tom *et al.,* 2007; Plassmann *et al.,* 2010). Similarly, our methods did not allow us to dissociate the coding of value and salience signals (Seeley *et al.,* 2007; Bressler and Menon, 2010), which are difficult to tease apart in many decision experiments. However, one study in our corpus dissociates these two signals (Litt *et al.,* 2011), finding that the regions of VMPFC and PCC identified in our meta-analyses are associated with value but not saliency coding, and that VSTR is associated with both types of computations. There is also evidence for non-linear (e.g. quadratic) responses to subjective measures of value in a handful of fMRI studies (O'Doherty *et al.,* 2006; Todorov *et al.,* 2011). Finally, our methods do not facilitate the delineation of regions that compute stimulus values from regions that compute reward prediction errors. This is an important limitation because these signals are highly correlated in many studies, a phenomenon that may also account for our common finding of reliable VMPFC and VSTR value signals at both decision and outcome. The few studies that have directly looked at separating these computations have found that VMPFC reflects values, whereas VSTR reflects prediction errors (Hare *et al.,* 2008; Rohe *et al.,* 2012).

Despite these limitations, the analyses presented here offer a clear set of brain regions that are reliably recruited to compute subjective value. Many of the regions in our results mirror components of established functional networks (Smith *et al.,* 2009; Andrews-Hanna *et al.,* 2010; Bressler and Menon, 2010). An important step in constructing a biologically plausible model of value computation in the brain (Clithero *et al.,* 2008; Fehr and Rangel, 2011; Glimcher, 2011) requires identifying accurate constraints on computations, and networks in the brain are one of those key constraints. Thus, the network of areas identified in our meta-analyses point to important open questions about the computation of subjective value that should be addressed in future fMRI studies. In this way, informatics can be employed to guide future studies of decision-making systems in the brain (Poldrack, 2010; Yarkoni *et al.*, 2010, 2011).

Conflict of interest

None declared.

REFERENCES

Anderson, A.K., Christoff, K., Stappen, I., et al. (2003). Dissociated neural representations of intensity and valence in human olfaction. *Nature Neuroscience*, *6*, 196–202.

Andrews-Hanna, J.R., Reidler, J.S., Sepulcre, J., Poulin, R., Buckner, R.L. (2010). Functional-anatomic fractionation of the brain's default network. *Neuron*, *65*, 550–62.

Basten, U., Biele, G., Heekeren, H.R., Fiebach, C.J. (2010). How the brain integrates costs and benefits during decision making. *Proceedings of the National Academy of Sciences, USA*, *107*, 21767–72.

Baumgartner, T., Knoch, D., Hotz, P., Eisenegger, C., Fehr, E. (2011). Dorsolateral and ventromedial prefrontal cortex orchestrate normative choice. *Nature Neuroscience*, *14*, 1468–74.

Beckmann, M., Johansen-Berg, H., Rushworth, M.F. (2009). Connectivity-based parcellation of human cingulate cortex and its relation to functional specialization. *Journal of Neuroscience*, *29*, 1175–90.

Behrens, T.E.J., Hunt, L.T., Woolrich, M.W., Rushworth, M.F.S. (2008). Associative learning of social value. *Nature*, *456*, 245–50.

Behrens, T.E., Johansen-Berg, H., Woolrich, M.W., et al. (2003). Non-invasive mapping of connections between human thalamus and cortex using diffusion imaging. *Nature Neuroscience*, *6*, 750–7.

Behrens, T.E., Woolrich, M.W., Walton, M.E., Rushworth, M.F. (2007). Learning the value of information in an uncertain world. *Nature Neuroscience*, *10*, 1214–21.

Boorman, E.D., Behrens, T.E., Woolrich, M.W., Rushworth, M.F. (2009). How green is the grass on the other side? Frontopolar cortex and the evidence in favor of alternative courses of action. *Neuron*, *62*, 733–43.

Bressler, S.L., Menon, V. (2010). Large-scale brain networks in cognition: emerging methods and principles. *Trends in Cognitive Science*, *14*, 277–90.

Brooks, A.M., Pammi, V.S., Noussair, C., Capra, C.M., Engelmann, J.B., Berns, G.S. (2010). From bad to worse: striatal coding of the relative value of painful decisions. *Frontiers in Neuroscience*, *4*, 176.

Buckner, R.L., Andrews-Hanna, J.R., Schacter, D.L. (2008). The brain's default network: anatomy, function, and relevance to disease. *Annals of the New York Academy of Sciences*, *1124*, 1–38.

Carmichael, S.T., Price, J.L. (1995). Sensory and premotor connections of the orbital and medial prefrontal cortex of macaque monkeys. *The Journal of Comparative Neurology*, *363*, 642–64.

Carter, R.M., Meyer, J.R., Huettel, S.A. (2010). Functional neuroimaging of intertemporal choice models: a review. *Journal of Neuroscience, Psychology, and Economics*, *3*, 27–45.

Cauda, F., Cavanna, A.E., D'Agata, F., Sacco, K., Duca, S., Geminiani, G.C. (2011). Functional connectivity and coactivation of the nucleus accumbens: a combined functional connectivity and structure-based meta-analysis. *Journal of Cognitive Neuroscience*, *23*, 2864–77.

Chib, V.S., Rangel, A., Shimojo, S., O'Doherty, J.P. (2009). Evidence for a common representation of decision values for dissimilar goods in human ventromedial prefrontal cortex. *Journal of Neuroscience*, *29*, 12315–20.

Clithero, J.A., Tankersley, D., Huettel, S.A. (2008). Foundations of neuroeconomics: from philosophy to practice. *PLoS Biol*, *6*, e298.

Cloutier, J., Heatherton, T.F., Whalen, P.J., Kelley, W.M. (2008). Are attractive people rewarding? Sex differences in the neural substrates of facial attractiveness. *Journal of Cognitive Neuroscience*, *20*, 941–51.

Cohen, M.X. (2007). Individual differences and the neural representations of reward expectation and reward prediction error. *Social Cognitive and Affective Neuroscience*, *2*, 20–30.

Croxson, P.L., Walton, M.E., O'Reilly, J.X., Behrens, T.E., Rushworth, M.F. (2009). Effort-based cost-benefit valuation and the human brain. *Journal of Neuroscience*, *29*, 4531–41.

Daw, N.D., O'Doherty, J.P., Dayan, P., Seymour, B., Dolan, R.J. (2006). Cortical substrates for exploratory decisions in humans. *Nature*, *441*, 876–9.

de Araujo, I.E., Kringelbach, M.L., Rolls, E.T., McGlone, F. (2003). Human cortical responses to water in the mouth, and the effects of thirst. *Journal of Neurophysiology*, *90*, 1865–76.

de Araujo, I.E., Rolls, E.T., Velazco, M.I., Margot, C., Cayeux, I. (2005). Cognitive modulation of olfactory processing. *Neuron*, *46*, 671–9.

De Martino, B., Kumaran, D., Holt, B., Dolan, R.J. (2009). The neurobiology of reference-dependent value computation. *Journal of Neuroscience*, *29*, 3833–42.

Eickhoff, S.B., Laird, A.R., Grefkes, C., Wang, L.E., Zilles, K., Fox, P.T. (2009). Coordinate-based activation likelihood estimation meta-analysis of neuroimaging data: A random-effects approach based on empirical estimates of spatial uncertainty. *Human Brain Mapping*, *30*, 2907–26.

Eickhoff, S.B., Bzdok, D., Laird, A.R., Kurth, F., Fox, P.T. (2012). Activation likelihood estimation meta-analysis revisited. *Neuroimage*, *59*, 2349–61.

Eickhoff, S.B., Bzdok, D., Laird, A.R., et al. (2011). Co-activation patterns distinguish cortical modules, their connectivity and functional differentiation. *Neuroimage*, *57*, 938–49.

Fehr, E., Rangel, A. (2011). Neuroeconomic foundations of economic choice - recent advances. *Journal of Economic Perspectives*, *25*, 3–30.

FitzGerald, T.H., Seymour, B., Bach, D.R., Dolan, R.J. (2010). Differentiable neural substrates for learned and described value and risk. *Current Biology*, *20*, 1823–9.

FitzGerald, T.H., Seymour, B., Dolan, R.J. (2009). The role of human orbitofrontal cortex in value comparison for incommensurable objects. *Journal of Neuroscience*, *29*, 8388–95.

Fox, P.T., Friston, K.J. (2012). Distributed processing; distributed functions? *Neuroimage*, *61*, 407–26.

Friston, K.J. (2007). *Statistical Parametric Mapping : The Analysis of Funtional Brain Images.* Amsterdam, Boston: Elsevier/Academic Press, pp. 647.

Gilbert, S.J., Gonen-Yaacovi, G., Benoit, R.G., Volle, E., Burgess, P.W. (2010). Distinct functional connectivity associated with lateral versus medial rostral prefrontal cortex: a meta-analysis. *Neuroimage*, *53*, 1359–67.

Glascher, J., Hampton, A.N., O'Doherty, J.P. (2009). Determining a role for ventromedial prefrontal cortex in encoding action-based value signals during reward-related decision making. *Cerebral Cortex*, *19*, 483–95.

Glimcher, P.W. (2011). *Foundations of Neuroeconomic Analysis.* Oxford, New York: Oxford University Press.

Gottfried, J.A., O'Doherty, J., Dolan, R.J. (2003). Encoding predictive reward value in human amygdala and orbitofrontal cortex. *Science*, *301*, 1104–7.

Grabenhorst, F., D'Souza, A.A., Parris, B.A., Rolls, E.T., Passingham, R.E. (2010). A common neural scale for the subjective pleasantness of different primary rewards. *Neuroimage*, *51*, 1265–74.

Grabenhorst, F., Rolls, E.T. (2009). Different representations of relative and absolute subjective value in the human brain. *Neuroimage*, *48*, 258–68.

Grabenhorst, F., Rolls, E.T. (2011). Value, pleasure and choice in the ventral prefrontal cortex. *Trends in Cognitive Science*, *15*, 56–67.

Hampton, A.N., Bossaerts, P., O'Doherty, J.P. (2006). The role of the ventromedial prefrontal cortex in abstract state-based inference during decision making in humans. *Journal of Neuroscience*, *26*, 8360–7.

Hare, T.A., Camerer, C.F., Knoepfle, D.T., Rangel, A. (2010). Value computations in ventral medial prefrontal cortex during charitable decision making incorporate input from regions involved in social cognition. *Journal of Neuroscience*, *30*, 583–90.

Hare, T.A., Camerer, C.F., Rangel, A. (2009). Self-control in decision-making involves modulation of the vmPFC valuation system. *Science*, *324*, 646–8.

Hare, T.A., Malmaud, J., Rangel, A. (2011a). focusing attention on the health aspects of foods changes value signals in vmPFC and improves dietary choice. *Journal of Neuroscience*, *31*, 11077–87.

Hare, T.A., O'Doherty, J., Camerer, C.F., Schultz, W., Rangel, A. (2008). Dissociating the role of the orbitofrontal cortex and the striatum in the computation of goal values and prediction errors. *Journal of Neuroscience*, *28*, 5623–30.

Hare, T.A., Schultz, W., Camerer, C.F., O'Doherty, J.P., Rangel, A. (2011b). Transformation of stimulus value signals into motor commands during simple choice. *Proceedings of the National Academy of Sciences, USA*, *108*, 18120–5.

Hayden, B.Y., Platt, M.L. (2010). Neurons in anterior cingulate cortex multiplex information about reward and action. *Journal of Neuroscience*, *30*, 3339–46.

Heekeren, H.R., Marrett, S., Bandettini, P.A., Ungerleider, L.G. (2004). A general mechanism for perceptual decision-making in the human brain. *Nature*, *431*, 859–62.

Hsu, M., Krajbich, I., Zhao, C., Camerer, C.F. (2009). Neural response to reward anticipation under risk is nonlinear in probabilities. *Journal of Neuroscience*, *29*, 2231–7.

Hutcherson, C., Plassmann, H., Gross, J.J., Rangel, A. (2012). Cognitive regulation during decision making shifts behavioral control between ventromedial and dorsolateral prefrontal value systems. *Journal of Neuroscience*, *32*, 13543–54.

Izuma, K., Matsumoto, M., Murayama, K., Samejima, K., Sadato, N., Matsumoto, K. (2010). Neural correlates of cognitive dissonance and choice-induced preference change. *Proceedings of the National Academy of Sciences, USA*, *107*, 22014–9.

Janowski, V., Camerer, C., Rangel, A. (2013). Empathic choice involves vmPFC value signals that are modulated by social processing implemented in IPL. *Social Cognitive and Affective Neuroscience*, *8*, 201–8.

Jocham, G., Hunt, L.T., Near, J., Behrens, T.E. (2012). A mechanism for value-guided choice based on the excitation-inhibition balance in prefrontal cortex. *Nature Neuroscience*, *15*, 960–1.

Jocham, G., Klein, T.A., Ullsperger, M. (2011). Dopamine-mediated reinforcement learning signals in the striatum and ventromedial prefrontal cortex underlie value-based choices. *Journal of Neuroscience*, *31*, 1606–13.

Kable, J.W., Glimcher, P.W. (2007). The neural correlates of subjective value during intertemporal choice. *Nature Neuroscience*, *10*, 1625–33.

Kable, J.W., Glimcher, P.W. (2010). An "as soon as possible" effect in human intertemporal decision making: behavioral evidence and neural mechanisms. *Journal of Neurophysiology*, *103*, 2513–31.

Kahnt, T., Chang, L.J., Park, S.Q., Heinzle, J., Haynes, J.D. (2012). Connectivity-based parcellation of the human orbitofrontal cortex. *Journal of Neuroscience*, *32*, 6240–50.

Kang, M.J., Rangel, A., Camus, M., Camerer, C.F. (2011). Hypothetical and real choice differentially activate common valuation areas. *Journal of Neuroscience*, *31*, 461–8.

Kennerley, S.W., Dahmubed, A.F., Lara, A.H., Wallis, J.D. (2009). Neurons in the frontal lobe encode the value of multiple decision variables. *Journal of Cognitive Neuroscience*, *21*, 1162–78.

Kim, H., Shimojo, S., O'Doherty, J.P. (2006). Is avoiding an aversive outcome rewarding? Neural substrates of avoidance learning in the human brain. *PLoS Biology*, *4*, e233.

Kim, H., Shimojo, S., O'Doherty, J.P. (2011). Overlapping responses for the expectation of juice and money rewards in human ventromedial prefrontal cortex. *Cerebral Cortex*, *21*, 769–76.

Knutson, B., Rick, S., Wimmer, G.E., Prelec, D., Loewenstein, G. (2007). Neural predictors of purchases. *Neuron*, *53*, 147–56.

Kober, H., Wager, T.D. (2010). Meta-analysis of neuroimaging data. *WIREs Cognitive Science*, *1*, 293–300.

Koeneke, S., Pedroni, A.F., Dieckmann, A., Bosch, V., Jancke, L. (2008). Individual preferences modulate incentive values: Evidence from functional MRI. *Behavioral and Brain Functions*, *4*, 55.

Kringelbach, M.L., Rolls, E.T. (2004). The functional neuroanatomy of the human orbitofrontal cortex: evidence from neuroimaging and neuropsychology. *Progress in Neurobiology*, *72*, 341–72.

Kringelbach, M.L., O'Doherty, J., Rolls, E.T., Andrews, C. (2003). Activation of the human orbitofrontal cortex to a liquid food stimulus is correlated with its subjective pleasantness. *Cerebral Cortex*, *13*, 1064–71.

Kuhn, S., Gallinat, J. (2012). The neural correlates of subjective pleasantness. *Neuroimage*, *61*, 289–94.

Laird, A.R., Fox, P.M., Price, C.J., et al. (2005). ALE meta-analysis: controlling the false discovery rate and performing statistical contrasts. *Human Brain Mapping*, *25*, 155–64.

Lancaster, J.L., Tordesillas-Gutierrez, D., Martinez, M., et al. (2007). Bias between MNI and Talairach coordinates analyzed using the ICBM-152 brain template. *Human Brain Mapping*, *28*, 1194–205.

Lazar, N.A., Luna, B., Sweeney, J.A., Eddy, W.F. (2002). Combining brains: a survey of methods for statistical pooling of information. *Neuroimage*, *16*, 538–50.

Lebreton, M., Jorge, S., Michel, V., Thirion, B., Pessiglione, M. (2009). An automatic valuation system in the human brain: evidence from functional neuroimaging. *Neuron*, *64*, 431–9.

Leech, R., Kamourieh, S., Beckmann, C.F., Sharp, D.J. (2011). Fractionating the default mode network: distinct contributions of the ventral and dorsal posterior cingulate cortex to cognitive control. *Journal of Neuroscience*, *31*, 3217–24.

Levy, D.J., Glimcher, P.W. (2011). Comparing apples and oranges: using reward-specific and reward-general subjective value representation in the brain. *Journal of Neuroscience*, *31*, 14693–707.

Levy, D.J., Glimcher, P.W. (2012). The root of all value: a neural common currency for choice. *Current Opinion in Neurobiology*, *22*, 1027–38.

Levy, I., Snell, J., Nelson, A.J., Rustichini, A., Glimcher, P.W. (2010). Neural representation of subjective value under risk and ambiguity. *Journal of Neurophysiology*, *103*, 1036–47.

Lim, S.L., O'Doherty, J.P., Rangel, A. (2011). The decision value computations in the vmPFC and striatum use a relative value code that is guided by visual attention. *Journal of Neuroscience*, *31*, 13214–23.

Lin, A., Adolphs, R., Rangel, A. (2012). Social and monetary reward learning engage overlapping neural substrates. *Social Cognitive and Affective Neuroscience*, *7*, 274–81.

Litt, A., Plassmann, H., Shiv, B., Rangel, A. (2011). Dissociating valuation and saliency signals during decision-making. *Cerebral Cortex*, *21*, 95–102.

Liu, L., Feng, T., Wang, J., Li, H. (2012). The neural dissociation of subjective valuation from choice processes in intertemporal choice. *Behavioural Brain Research*, *231*, 40–7.

Liu, X., Hairston, J., Schrier, M., Fan, J. (2011). Common and distinct networks underlying reward valence and processing stages: a meta-analysis of functional neuroimaging studies. *Neuroscience and Biobehavioral Reviews*, *35*, 1219–36.

Mars, R.B., Neubert, F.X., Noonan, M.P., Sallet, J., Toni, I., Rushworth, M.F. (2012). On the relationship between the "default mode network" and the "social brain". *Frontiers in Human Neuroscience*, *6*, 189.

McClure, S.M., Li, J., Tomlin, D., Cypert, K.S., Montague, L.M., Montague, P.R. (2004). Neural correlates of behavioral preference for culturally familiar drinks. *Neuron*, *44*, 379–87.

McNamee, D., Rangel, A., O'Doherty, J.P. (2013). Category-dependent and category-independent goal-value codes in human ventromedial prefrontal cortex. *Nature Neuroscience*, *16*, 479–85.

Mohr, P.N., Biele, G., Heekeren, H.R. (2010). Neural processing of risk. *Journal of Neuroscience*, *30*, 6613–9.

Nakao, T., Ohira, H., Northoff, G. (2012). Distinction between externally vs. internally guided decision-making: operational differences, meta-analytical comparisons and their theoretical implications. *Frontiers in Neuroscience*, *6*, 31.

O'Doherty, J.P. (2011). Contributions of the ventromedial prefrontal cortex to goal-directed action selection. *Annals of the New York Academy of Sciences*, *1239*, 118–29.

O'Doherty, J.P., Buchanan, T.W., Seymour, B., Dolan, R.J. (2006). Predictive neural coding of reward preference involves dissociable responses in human ventral midbrain and ventral striatum. *Neuron*, *49*, 157–66.

Padoa-Schioppa, C. (2011). Neurobiology of economic choice: a good-based model. *Annual Review of Neuroscience*, *34*, 333–59.

Park, S.Q., Kahnt, T., Rieskamp, J., Heekeren, H.R. (2011). Neurobiology of value integration: when value impacts valuation. *Journal of Neuroscience*, *31*, 9307–14.

Pearson, J.M., Heilbronner, S.R., Barack, D.L., Hayden, B.Y., Platt, M.L. (2011). Posterior cingulate cortex: adapting behavior to a changing world. *Trends in Cognitive Science*, *15*, 143–51.

Peters, J., Buchel, C. (2009). Overlapping and distinct neural systems code for subjective value during intertemporal and risky decision making. *Journal of Neuroscience*, *29*, 15727–34.

Peters, J., Buchel, C. (2010a). Episodic future thinking reduces reward delay discounting through an enhancement of prefrontal-mediotemporal interactions. *Neuron*, *66*, 138–48.

Peters, J., Buchel, C. (2010b). Neural representations of subjective reward value. *Behavioural Brain Research*, *213*, 135–41.

Pine, A., Seymour, B., Roiser, J.P., et al. (2009). Encoding of marginal utility across time in the human brain. *Journal of Neuroscience*, *29*, 9575–81.

Pine, A., Shiner, T., Seymour, B., Dolan, R.J. (2010). Dopamine, time, and impulsivity in humans. *Journal of Neuroscience*, *30*, 8888–96.

Plassmann, H., O'Doherty, J., Rangel, A. (2007). Orbitofrontal cortex encodes willingness to pay in everyday economic transactions. *Journal of Neuroscience*, *27*, 9984–88.

Plassmann, H., O'Doherty, J., Shiv, B., Rangel, A. (2008). Marketing actions can modulate neural representations of experienced pleasantness. *Proceedings of the National Academy of Sciences, USA*, *105*, 1050–4.

Plassmann, H., O'Doherty, J.P., Rangel, A. (2010). Appetitive and aversive goal values are encoded in the medial orbitofrontal cortex at the time of decision making. *Journal of Neuroscience*, *30*, 10799–808.

Poldrack, R.A. (2010). Mapping mental function to brain structure: how can cognitive neuroimaging succeed? *Perspectives on Psychological Science*, *5*, 753–61.

Prevost, C., Pessiglione, M., Metereau, E., Clery-Melin, M.L., Dreher, J.C. (2010). Separate valuation subsystems for delay and effort decision costs. *Journal of Neuroscience*, *30*, 14080–90.

Price, J.L., Drevets, W.C. (2010). Neurocircuitry of mood disorders. *Neuropsychopharmacology*, *35*, 192–216.

Rangel, A., Camerer, C., Montague, P.R. (2008). A framework for studying the neurobiology of value-based decision making. *Nature Reviews Neuroscience*, *9*, 545–56.

Rangel, A., Hare, T. (2010). Neural computations associated with goal-directed choice. *Current Opinion in Neurobiology*, *20*, 262–70.

Rohe, T., Weber, B., Fliessbach, K. (2012). Dissociation of BOLD responses to reward prediction errors and reward receipt by a model comparison. *European Journal of Neuroscience*, *36*, 2376–82.

Rolls, E.T. (2000). Neurophysiology and functions of the primate amygdala, and the neural basis of emotion. *The Amygdala: A Functional Analysis*, pp. 447–78.

Rolls, E.T., Grabenhorst, F. (2008). The orbitofrontal cortex and beyond: from affect to decision-making. *Progress in Neurobiology*, *86*, 216–44.

Rolls, E.T., Grabenhorst, F., Parris, B.A. (2008). Warm pleasant feelings in the brain. *Neuroimage*, *41*, 1504–13.

Rolls, E.T., Grabenhorst, F., Parris, B.A. (2010). Neural systems underlying decisions about affective odors. *Journal of Cognitive Neuroscience*, *22*, 1069–82.

Rolls, E.T., McCabe, C. (2007). Enhanced affective brain representations of chocolate in cravers vs. *non-cravers. European Journal of Neuroscience*, *26*, 1067–76.

Rorden, C., Karnath, H.O., Bonilha, L. (2007). Improving lesion-symptom mapping. *Journal of Cognitive Neuroscience*, *19*, 1081–88.

Roy, M., Shohamy, D., Wager, T.D. (2012). Ventromedial prefrontal-subcortical systems and the generation of affective meaning. *Trends in Cognitive Science*, *16*, 147–56.

Rushworth, M.F., Noonan, M.P., Boorman, E.D., Walton, M.E., Behrens, T.E. (2011). Frontal cortex and reward-guided learning and decision-making. *Neuron*, *70*, 1054–69.

Salimi-Khorshidi, G., Smith, S.M., Keltner, J.R., Wager, T.D., Nichols, T.E. (2009). Meta-analysis of neuroimaging data: a comparison of image-based and coordinate-based pooling of studies. *Neuroimage*, *45*, 810–23.

Schacter, D.L., Addis, D.R., Buckner, R.L. (2007). Remembering the past to imagine the future: the prospective brain. *Nature Reviews Neuroscience*, *8*, 657–61.

Seeley, W.W., Menon, V., Schatzberg, A.F., et al. (2007). Dissociable intrinsic connectivity networks for salience processing and executive control. *Journal of Neuroscience*, *27*, 2349–56.

Serences, J.T. (2008). Value-based modulations in human visual cortex. *Neuron*, *60*, 1169–81.

Sescousse, G., Redoute, J., Dreher, J.C. (2010). The architecture of reward value coding in the human orbitofrontal cortex. *Journal of Neuroscience*, *30*, 13095–104.

Seymour, B., Dolan, R. (2008). Emotion, decision making, and the amygdala. *Neuron*, *58*, 662–71.

Shenhav, A., Greene, J.D. (2010). Moral judgments recruit domain-general valuation mechanisms to integrate representations of probability and magnitude. *Neuron*, *67*, 667–77.

Simon, D.A., Daw, N.D. (2011). Neural correlates of forward planning in a spatial decision task in humans. *Journal of Neuroscience*, *31*, 5526–39.

Smith, D.V., Hayden, B.Y., Truong, T.K., Song, A.W., Platt, M.L., Huettel, S.A. (2010). Distinct value signals in anterior and posterior ventromedial prefrontal cortex. *Journal of Neuroscience*, *30*, 2490–5.

Smith, S.M., Fox, P.T., Miller, K.L., et al. (2009). Correspondence of the brain's functional architecture during activation and rest. *Proceedings of the National Academy of Sciences, USA*, *106*, 13040–5.

Sokol-Hessner, P., Hutcherson, C., Hare, T., Rangel, A. (2012). Decision value computation in DLPFC and VMPFC adjusts to the available decision time. *European Journal of Neuroscience*, *35*, 1065–74.

Sripada, C.S., Gonzalez, R., Phan, K.L., Liberzon, I. (2011). The neural correlates of intertemporal decision-making: contributions of subjective value, stimulus type, and trait impulsivity. *Human Brain Mapping*, *32*, 1637–48.

Studer, B., Apergis-Schoute, A.M., Robbins, T.W., Clark, L. (2012). What are the odds? The neural correlates of active choice during gambling. *Frontiers in Neuroscience*, *6*, 46.

Summerfield, C., Koechlin, E. (2010). Economic value biases uncertain perceptual choices in the parietal and prefrontal cortices. *Frontiers in Human Neuroscience*, *4*, 208.

Suzuki, S., Harasawa, N., Ueno, K., Gardner, J.L., et al. (2012). Learning to simulate others' decisions. *Neuron*, *74*, 1125–37.

Symmonds, M., Bossaerts, P., Dolan, R.J. (2010). A behavioral and neural evaluation of prospective decision-making under risk. *Journal of Neuroscience*, *30*, 14380–9.

Tanaka, S.C., Doya, K., Okada, G., Ueda, K., Okamoto, Y., Yamawaki, S. (2004). Prediction of immediate and future rewards differentially recruits cortico-basal ganglia loops. *Nature Neuroscience*, *7*, 887–93.

Tobler, P.N., O'Doherty, J.P., Dolan, R.J., Schultz, W. (2007). Reward value coding distinct from risk attitude-related uncertainty coding in human reward systems. *Journal of Neurophysiology*, *97*, 1621–32.

Todorov, A., Said, C.P., Oosterhof, N.N., Engell, A.D. (2011). Task-invariant brain responses to the social value of faces. *Journal of Cognitive Neuroscience*, *23*, 2766–81.

Tom, S.M., Fox, C.R., Trepel, C., Poldrack, R.A. (2007). The neural basis of loss aversion in decision-making under risk. *Science*, *315*, 515–8.

Toro, R., Fox, P.T., Paus, T. (2008). Functional coactivation map of the human brain. *Cerebral Cortex*, *18*, 2553–9.

Turkeltaub, P.E., Eickhoff, S.B., Laird, A.R., Fox, M., Wiener, M., Fox, P. (2012). Minimizing within-experiment and within-group effects in Activation Likelihood Estimation meta-analyses. *Human Brain Mapping*, *33*, 1–13.

Venkatraman, V., Rosati, A.G., Taren, A.A., Huettel, S.A. (2009). Resolving response, decision, and strategic control: evidence for a functional topography in dorsomedial prefrontal cortex. *Journal of Neuroscience*, *29*, 13158–64.

Wager, T.D., Lindquist, M., Kaplan, L. (2007). Meta-analysis of functional neuroimaging data: current and future directions. *Social Cognitive and Affective Neuroscience*, *2*, 150–8.

Wager, T.D., Phan, K.L., Liberzon, I., Taylor, S.F. (2003). Valence, gender, and lateralization of functional brain anatomy in emotion: a meta-analysis of findings from neuroimaging. *Neuroimage*, *19*, 513–31.

Wallis, J.D. (2012). Cross-species studies of orbitofrontal cortex and value-based decision-making. *Nature Neuroscience*, *15*, 13–9.

Wallis, J.D., Kennerley, S.W. (2010). Heterogeneous reward signals in prefrontal cortex. *Current Opinion in Neurobiology*, *20*, 191–8.

Walter, M., Bermpohl, F., Mouras, H., et al. (2008). Distinguishing specific sexual and general emotional effects in fMRI-subcortical and cortical arousal during erotic picture viewing. *Neuroimage*, *40*, 1482–94.

Wimmer, G.E., Daw, N.D., Shohamy, D. (2012). Generalization of value in reinforcement learning by humans. *European Journal of Neuroscience*, *35*, 1092–104.

Winston, J.S., O'Doherty, J., Kilner, J.M., Perrett, D.I., Dolan, R.J. (2007). Brain systems for assessing facial attractiveness. *Neuropsychologia*, *45*, 195–206.

Woolrich, M.W., Jbabdi, S., Patenaude, B., et al. (2009). Bayesian analysis of neuroimaging data in FSL. *Neuroimage*, *45*, S173–86.

Wu, S.W., Delgado, M.R., Maloney, L.T. (2011). The neural correlates of subjective utility of monetary outcome and probability weight in economic and in motor decision under risk. *Journal of Neuroscience*, *31*, 8822–31.

Wunderlich, K., Dayan, P., Dolan, R.J. (2012). Mapping value based planning and extensively trained choice in the human brain. *Nature Neuroscience*, *15*, 786–91.

Wunderlich, K., Rangel, A., O'Doherty, J.P. (2009). Neural computations underlying action-based decision making in the human brain. *Proceedings of the National Academy of Sciences, USA*, *106*, 17199–204.

Wunderlich, K., Rangel, A., O'Doherty, J.P. (2010). Economic choices can be made using only stimulus values. *Proceedings of the National Academy of Sciences, USA*, *107*, 15005–10.

Xue, G., Lu, Z., Levin, I.P., Weller, J.A., Li, X., Bechara, A. (2009). Functional dissociations of risk and reward processing in the medial prefrontal cortex. *Cerebral Cortex*, *19*, 1019–27.

Yarkoni, T., Poldrack, R.A., Nichols, T.E., Van Essen, D.C., Wager, T.D. (2011). Large-scale automated synthesis of human functional neuroimaging data. *Nature Methods*, *8*, 665–70.

Yarkoni, T., Poldrack, R.A., Van Essen, D.C., Wager, T.D. (2010). Cognitive neuroscience 2.0: building a cumulative science of human brain function. *Trends in Cognitive Science*, *14*, 489–96.